Chapter 1: Signal and Linear System Analysis

Signals can be classified according to attributes. A few such classifications are outlined below.

1) A *deterministic signal* can be specified as a function of time by a mathematical formula. At any instant of time t, x(t) is a number. For example, x(t) = A$\cos\omega t$ is a deterministic signal.

2. *Random signals* take on random values at any given time; at time t, random signal x(t) is a random variable, not a simple number. Random signals must be modeled probabilistically using random process theory.

3. *Periodic signals* are deterministic signals for which

$$x(t) = x(t+T), \; -\infty<t<\infty, \tag{1-1}$$

where T is a constant. The smallest such T is called the *period* of x.

4. *Aperiodic signals* are deterministic signals that are not periodic. Usually, they are nonzero only over a finite length of time. The commonly-used single pulse is a simple example of an aperiodic signal.

Dirac Delta Function

The *Dirac Delta* function is denoted as δ(t), and it is defined by the property

$$\int_{-\infty}^{\infty} x(t)\delta(t)dt = x(0), \tag{1-2}$$

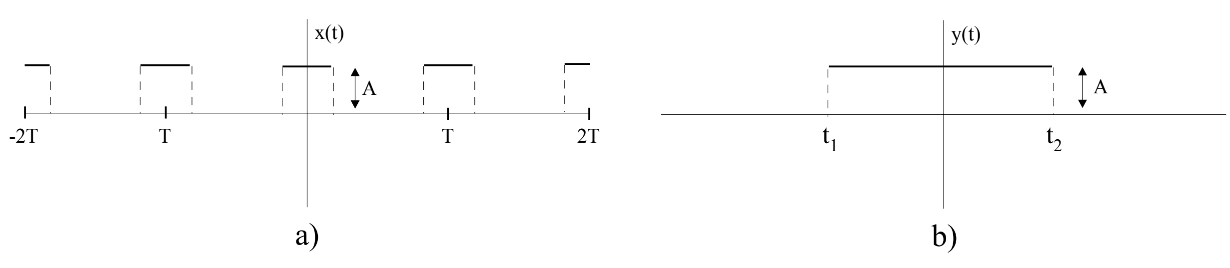

Figure 1-1: a) Periodic signal with period T. b) Aperiodic signal.

where x(t) is any function that is continuous at the origin. The delta function is only defined in terms of what it does to integrals (it only appears under an integral sign). In (1-2), a simple change of variable produces

$$\int_{-\infty}^{\infty} x(t)\delta(t-t_0)dt = x(t_0), \tag{1-3}$$

where it is assumed that x(t) is continuous at t_0. Formula (1-3) is called the *sifting property* of the delta function. Other properties of the delta function are listed below.

$$\delta(at) = \frac{1}{|a|}\delta(t) \tag{1-4}$$

$$\delta(-t) = \delta(t) \tag{1-5}$$

$$\int_{t_1}^{t_2} x(t)\delta(t-t_0)dt = \begin{cases} x(t_0), & t_1 < t_0 < t_2 \\ 0, & \text{otherwise} \end{cases} \tag{1-6}$$

$$x(t)\delta(t-t_0) = x(t_0)\delta(t-t_0) \tag{1-7}$$

$$\int_{t_1}^{t_2} x(t)\delta^{(n)}(t-t_0)dt = (-1)^n x^{(n)}(0), \quad t_1 < t_0 < t_2 \tag{1-8}$$

In (1-8), the quantity $x^{(n)}(t)$ denotes the n^{th} derivative of x; function x(t) and its first n derivatives are assumed to be continuous at $t = t_0$. $\delta^{(n)}$ is often called the *n^{th} generalized derivative* of δ.

The delta function can be thought of as the limit of a suitably chosen "conventional" function having unity area in an infinitesimally small width. Figure 1-2 illustrates three commonly used approximations. The first is a rectangular pulse of width 2ε and height of 1/2ε. It behaves like a delta function because

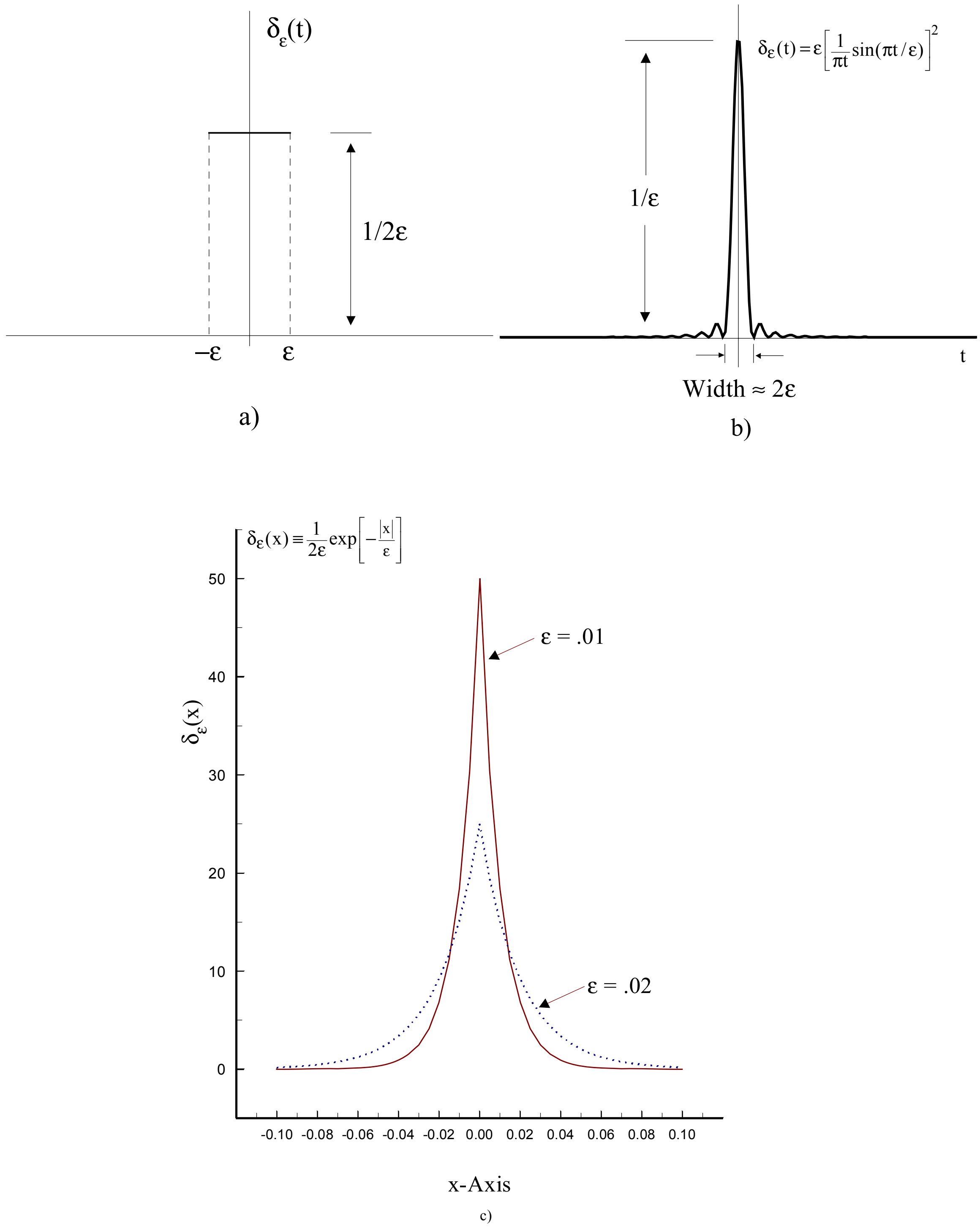

Figure 1-2: Three commonly-used approximations to the delta function.

$$\lim_{\varepsilon \to 0} \int_{-\infty}^{\infty} \delta_\varepsilon(t)x(t)\,dt = \lim_{\varepsilon \to 0}\left[(2\varepsilon)/(2\varepsilon)\right]x(0) = x(0) \tag{1-9}$$

for any x(t) that is continuous at t = 0. The approximation depicted by Figure 1-2b is given by

$$\delta_\varepsilon(t) = \varepsilon\left[\frac{1}{\pi t}\sin(\pi t/\varepsilon)\right]^2 = \frac{1}{\varepsilon}\left[\mathrm{Sa}(\pi t/\varepsilon)\right]^2, \tag{1-10}$$

where Sa(x) = {sin(x)}/x. As $\varepsilon \to 0$, function (1-10) becomes a delta function. Finally, Figure 1-2c depicts the approximation

$$\delta_\varepsilon(t) = \frac{1}{2\varepsilon}\exp\left[-\frac{|t|}{\varepsilon}\right]. \tag{1-11}$$

All three approximations are of unit area, independent of $\varepsilon > 0$.

Unit Step Function

The *unit step* function is denoted as U(t), and it is defined as

$$U(t) = \begin{cases} 0, & t < 0 \\ 1 & t > 0 \end{cases}. \tag{1-12}$$

The unit step is related to the delta function by the relationship

$$U(t) = \int_{-\infty}^{t} \delta(x)dx \tag{1-13}$$

$$\delta(t) = \frac{dU(t)}{dt}. \tag{1-14}$$

The unit step has many uses. For example, it can be used to construct complicated functions from simple pieces. Figure 1-3 illustrates a function that can be constructed from delayed ramps. Unit step functions can be used to describe this function as

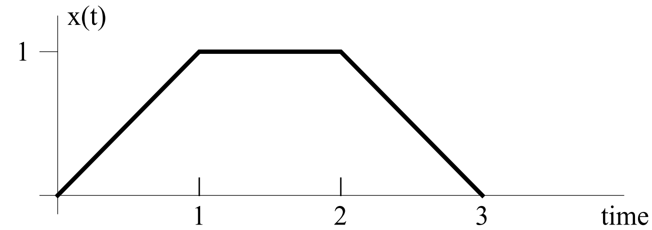

Figure 1-3: Simple signal that can be synthesized using ramps.

$$U(t) = tU(t) - (t-1)U(t-1) - (t-2)U(t-2) + (t-3)U(t-3)\,. \tag{1-15}$$

Energy and Power Signals

The total *energy on a per-ohm basis* in the complex-valued signal x(t) is defined as

$$E = \underset{T\to\infty}{\text{limit}} \int_{-T}^{T} |x(t)|^2\, dt\,. \tag{1-16}$$

The total *power on a per-ohm basis* in the complex-valued signal x(t) is defined as

$$P = \underset{T\to\infty}{\text{limit}} \frac{1}{2T} \int_{-T}^{T} |x(t)|^2\, dt\,. \tag{1-17}$$

x(t) is said to be an *energy signal* if $0 < E < \infty$ ($P = 0$ for an energy signal). And, x(t) is said to be a *power signal* if $0 < P < \infty$ ($E = \infty$ for a power signal).

Example 1-1: Consider $x(t) = Ae^{-\alpha t}\, U(t)$, $\alpha > 0$, where A and α are constants.

$$E = \int_0^\infty x^2(t)dt = \int_0^\infty A^2 e^{-2\alpha t} dt = \frac{A^2}{2\alpha} \tag{1-18}$$

x(t) is an energy signal.

Example 1-2: Consider $s(t) = A\cos(\omega t + \theta)$, where A, ω, and θ are constants. Compute

$$P = \lim_{T\to\infty} \frac{1}{2T}\int_{-T}^{T} A^2 \cos^2(\omega t + \theta)\, dt = \frac{A^2}{2}. \tag{1-19}$$

x(t) is a power signal since $0 < P < \infty$.

Generalized Fourier Series

Vector space concepts can be applied to signals. Recall the n-dimensional vector space $\mathcal{R}^n$. A vector $x \in \mathcal{R}^n$ can be represented as

$$x = \sum_{k=1}^{n} \xi_k \phi_k, \tag{1-20}$$

where vectors ϕ_k, $1 \le k \le n$, represent a basis for the space, and the ξ_k are constants. This basic idea extends to time-varying signals defined on an interval [0, T].

One can show that a vector space, called $L_2[0, T]$ here, can be defined which consists of all complex-valued signals x(t), $0 \le t \le T$, that satisfy

$$\int_0^T |x(t)|^2\, dt < \infty. \tag{1-21}$$

We use as scalars the field of complex numbers.

Let $\phi_k(t)$, $1 \le k \le n$, be a set of elements of space $L_2[0, T]$. Furthermore, require that they be *orthogonal*, which means

$$\begin{aligned} \int_0^T \phi_k(t)\phi_j^*(t)dt \quad &= c_k, \quad k = j \\ &= 0 \qquad k \ne j \end{aligned}, \tag{1-22}$$

where the c_k are real (nonzero) numbers. The orthogonal $\phi_k(t)$, $1 \le k \le n$, are said to *orthonormal* if $c_k = 1$, $1 \le k \le n$. Let x(t) be an arbitrary signal (*i.e.*, vector) in $L_2[0, T]$. Approximate x by the sum

$$x_a(t) = \sum_{k=1}^{n} \xi_k\, \phi_k(t)\,, \tag{1-23}$$

where ξ_k are scalars (complex numbers). Pick the ξ_k to minimize the integral square error (ISE)

$$\begin{aligned} e_n &\equiv \int_0^T \left|x_a(t) - x(t)\right|^2 dt = \int_0^T \left|\sum_{k=1}^{n} \xi_k\, \phi_k(t) - x(t)\right|^2 dt \\ &= \int_0^T |x(t)|^2\, dt - \sum_{k=1}^{n}\left[\xi_k^* \int_0^T x(t)\phi_k^*(t)dt + \xi_k \int_0^T x^*(t)\phi_k(t)dt\right] + \sum_{k=1}^{n} c_k\, |\xi_k|^2 \end{aligned} \tag{1-24}$$

The orthonormality of the ϕ_k ,and the ability to interchange integration and summation, have been used to produce (1-24). Now, by adding and subtracting a term, write (1-24) as

$$\begin{aligned} e_n &= \int_0^T |x(t)|^2\, dt \\ &\quad - \sum_{k=1}^{n}\left[\xi_k^* \int_0^T x(t)\phi_k^*(t)dt + \xi_k \int_0^T x^*(t)\phi_k(t)dt\right] + \sum_{k=1}^{n} c_k\, |\xi_k|^2 + \sum_{k=1}^{n} \frac{1}{c_k}\left|\int_0^T x(t)\phi_k^*(t)dt\right|^2, \\ &\quad - \sum_{k=1}^{n} \frac{1}{c_k}\left|\int_0^T x(t)\phi_k^*(t)dt\right|^2 \end{aligned} \tag{1-25}$$

which can be organized as (regroup the second line of (1-25))

$$e_n = \int_0^T |x(t)|^2\, dt + \sum_{k=1}^{n} c_k \left|\xi_k - \frac{1}{c_k}\int_0^T x(t)\phi_k^*(t)dt\right|^2 - \sum_{k=1}^{n} \frac{1}{c_k}\left|\int_0^T x(t)\phi_k^*(t)dt\right|^2. \tag{1-26}$$

Now, select the ξ_k to minimize the ISE e_n. Note that ξ_k only appears in the second term on the right hand side of (1-26). Also, this second term is always nonnegative (since the $c_k > 0$). Hence, to minimize ISE e_n, we should chose the ξ_k to "zero out" the second term. That is, take as the ξ_k the values

$$\xi_k = \frac{1}{c_k}\int_0^T x(t)\phi_k^*(t)dt\,, \tag{1-27}$$

$1 \le k \le n$. When these ξ_k are used, the minimum integral square error is

$$\min[e_n] = \int_0^T |x(t)|^2\,dt - \sum_{k=1}^{n}\frac{1}{c_k}\left|\int_0^T x(t)\phi_k^*(t)dt\right|^2 = \int_0^T |x(t)|^2\,dt - \sum_{k=1}^{n} c_k\,|\xi_k|^2\,. \tag{1-28}$$

There are infinite sets of basis functions for which the ISE is zero for all $x \in L_2[0, T]$. That is, there are infinite-dimensional sets of functions ϕ_k, $1 \le k < \infty$, for which

$$\underset{n\to\infty}{\text{limit}}\ \min[e_n] = 0 \tag{1-29}$$

and the *generalized Fourier series*

$$x(t) = \sum_{k=1}^{\infty}\xi_k\,\phi_k(t) \tag{1-30}$$

holds for all $x \in L_2[0, T]$. The ξ_k, defined by (1-27), are called *generalized Fourier coefficients*. Sets ϕ_k, $1 \le k < \infty$, of basis functions for which (1-29) holds for all $x \in L_2[0, T]$ are said to be *complete*.

It is very important to remember that the equality sign in (1-30) means *equality in the integral square error sense.* This is not the same as *pointwise equality*. As will be seen in the examples which follow, there can be values of t for which x(t) differs from the series expansion.

Suppose that an infinite-dimensional complete orthogonal sequence is used so that the ISE approaches zero as n approaches infinity. As a result, from (1-28) we get

$$\int_0^T |x(t)|^2\,dt = \sum_{k=1}^{\infty} c_k\,|\xi_k|^2\,, \tag{1-31}$$

a result known as *Parseval's theorem*.

Example 1-3: Consider the set of two orthonormal functions illustrated by Figure 1-4. Use these functions to compute a best integral-square-error approximation to the signal

$$x(t) = \begin{cases} \sin(\pi t), & 0 \le t \le 2 \\ 0, & \text{otherwise} \end{cases}. \tag{1-32}$$

Using (1-27), the coefficients are computed as

$$\begin{aligned} \xi_1 &= \int_0^2 \phi_1(t)\sin(\pi t)dt = \int_0^1 \sin(\pi t)dt = \frac{2}{\pi} \\ \xi_2 &= \int_0^2 \phi_2(t)\sin(\pi t)dt = \int_1^2 \sin(\pi t)dt = -\frac{2}{\pi}. \end{aligned} \tag{1-33}$$

Thus, the two-term approximation of x(t) is

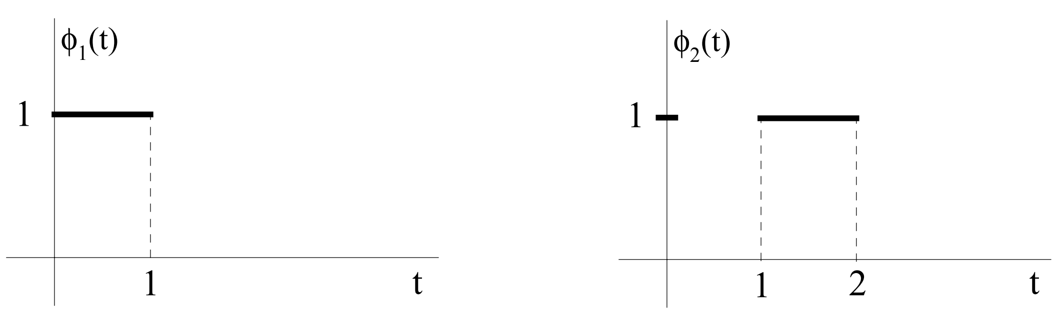

Figure 1-4: Two orthonormal functions.

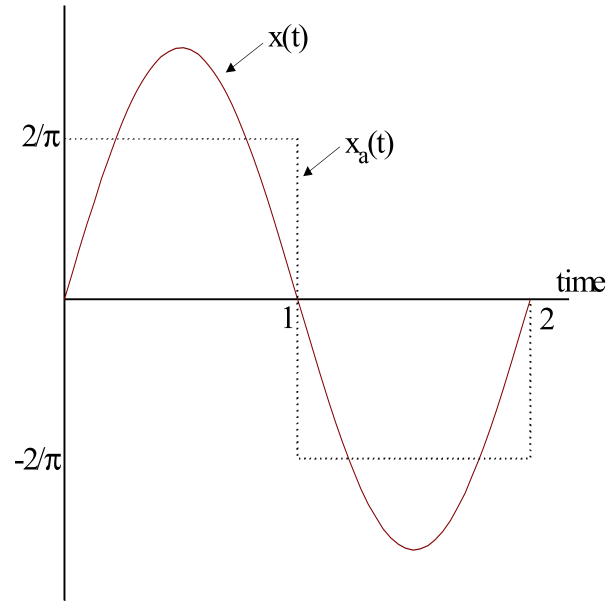

Figure 1-5: Sine wave and its two term approximation.

$$x_a(t) = \frac{2}{\pi}[\phi_1(t) - \phi_2(t)], \tag{1-34}$$

a result that is depicted by Figure 1-5. Finally, the ISE that results from the approximation is

$$\text{ISE} = \int_0^2 \sin^2(\pi t)dt - 2\left(\frac{2}{\pi}\right)^2 = 1 - \frac{8}{\pi^2} \approx .189 \tag{1-35}$$

Example 1-4: **Nyquist Low-Pass Sampling Theorem**

The Nyquist low-pass sampling theorem is an application of generalized Fourier Series. Here, we do not use space L_2 described above; instead, we use the signal space $\boldsymbol{V}$ of all signals x(t), $-\infty < t < \infty$, that are band-limited to **W** radians/sec. That is, space $\boldsymbol{V}$ consists of all signals x(t), $-\infty < t < \infty$, for which $|\mathcal{F}[x(t)]| = 0$ for $|\omega| \geq \mathbf{W}$ (verify that this is a valid vector space). We use basis functions of type {sin(x)}/x, and the Fourier coefficients are simply the signal samples $x(n\pi/\mathbf{W})$, $-\infty < n < \infty$.

Define

$$\phi_n(t) \equiv \mathrm{Sa}(\mathbf{W}t - n\pi), \; -\infty<n<\infty, \tag{1-36}$$

where Sa(x) = {sin(x)}/x. The Fourier transform of ϕ_n is

$$\mathcal{F}[\mathrm{Sa}(\mathbf{W}t - n\pi)] = \exp\{-j\frac{n\pi}{\mathbf{W}}\omega\}\left(\frac{\pi}{\mathbf{W}}\right)\mathrm{Rect}_{2\mathbf{W}}(\omega), \tag{1-37}$$

where Fig. 1-6 defines Π. Note that $\phi_n \in \boldsymbol{V}$ for all n. Without proof, we claim that the set of ϕ_n, -∞ < n < ∞, is *complete* in $\boldsymbol{V}$; any signal in $\boldsymbol{V}$ can be expanded in a Fourier series that represents the signal as a linear combination of the ϕ_n.

We show that the ϕ_n are orthogonal. By applying Parseval's theorem we can write

$$\int_{-\infty}^{\infty}\phi_n(t)\phi_m(t)dt = \frac{1}{2\pi}\int_{-\infty}^{\infty}\mathcal{F}[\phi_n(t)]\,\mathcal{F}[\phi_m(t)]^* d\omega. \tag{1-38}$$

Now, use (1-37) to obtain

$$\int_{-\infty}^{\infty}\mathrm{Sa}(\mathbf{W}t - n\pi)\mathrm{Sa}(\mathbf{W}t - m\pi)^* dt \quad = \frac{1}{2\pi}\int_{-\mathbf{W}}^{\mathbf{W}}\exp\left[-j(n-m)\frac{\pi}{\mathbf{W}}\omega\right]\left(\frac{\pi}{\mathbf{W}}\right)^2 d\omega, \tag{1-39}$$

or

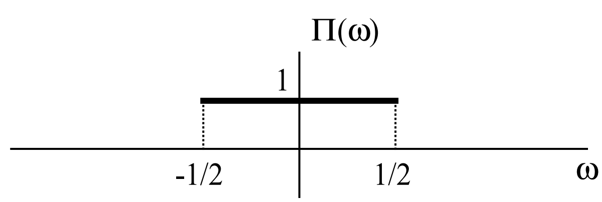

Figure 1-6: Graph of Π(ω).

$$\int_{-\infty}^{\infty} \mathrm{Sa}(\mathbf{W}t - n\pi)\mathrm{Sa}(\mathbf{W}t - m\pi)^* dt \begin{aligned} &= \frac{\pi}{\mathbf{W}}, \quad n = m \\ &= 0, \quad n \neq m \end{aligned}, \tag{1-40}$$

and the ϕ_n are orthogonal as claimed.

Now, use the ϕ_n as a set of basis functions. Let $x(t)$ be a bandlimited signal; that is, assume that $\mathbf{X}(\omega) = \mathcal{F}[x(t)] = 0$ for $|\omega| \geq \mathbf{W}$. Expand $x(t)$ in a Generalized Fourier Series using $\phi_n = \mathrm{Sa}(\mathbf{W}t - n\pi)$ as the basis functions. The generalized Fourier coefficients are

$$\xi_n = \frac{1}{(\pi/\mathbf{W})}\int_{-\infty}^{\infty} x(t)\mathrm{Sa}(\mathbf{W}t - n\pi)^* dt \tag{1-41}$$

Now, let $\mathbf{X}(\omega) = \mathcal{F}[x(t)]$, and use Parseval's theorem to write

$$\begin{aligned} \xi_n &= \frac{1}{(\pi/\mathbf{W})}\int_{-\infty}^{\infty} x(t)\mathrm{Sa}(\mathbf{W}t - n\pi)^* dt \\ &= \frac{1}{(\pi/\mathbf{W})}\frac{1}{2\pi}\int_{-\infty}^{\infty} \mathbf{X}(\omega)\left(\frac{\pi}{\mathbf{W}}\right)\exp\left[j\left(\frac{n\pi}{\mathbf{W}}\right)\omega\right]\mathrm{Rect}_{2\mathbf{W}}(\omega)\, d\omega \\ &= \frac{1}{2\pi}\int_{-\infty}^{\infty} \mathbf{X}(\omega)\exp\left[j\left(\frac{n\pi}{\mathbf{W}}\right)\omega\right] d\omega \ \ (\text{since } \mathbf{X}(\omega) = 0 \text{ for } |\omega| \geq \mathbf{W}) \\ &= x\left(\frac{n\pi}{\mathbf{W}}\right) \end{aligned} \tag{1-42}$$

Hence, *bandlimited* $x(t)$ *can be reconstructed from its samples by the generalized Fourier series*

$$x(t) = \sum_{n=-\infty}^{\infty} x\left(\frac{n\pi}{\mathbf{W}}\right)\mathrm{Sa}(\mathbf{W}t - n\pi). \tag{1-43}$$

This result is the well-known *Nyquist low-pass sampling theorem*, and it is simply an application of the theory of generalized Fourier series.

Exponential Fourier Series

Let x(t) be defined on the interval [0, T]. For the *exponential Fourier Series*, we use the complete orthogonal set $\phi_k = \exp[jk\omega_0 t]$, where $\omega_0 = 2\pi/T$. For these basis functions, we have

$$c_k = \int_0^T |e^{jk\omega_0 t}|^2 dt = T\,, \tag{1-44}$$

so that

$$x(t) = \sum_{k=-\infty}^{\infty} \zeta_k e^{jk\omega_0 t}\,, \tag{1-45}$$

where

$$\zeta_k = \frac{1}{T}\int_0^T x(t)e^{-jk\omega_0 t}dt\,, \tag{1-46}$$

and $\omega_0 = 2\pi/T$. Series (1-45) represents x(t) on the interval [0, T]; if x(t) is T-periodic, the series represents x(t) on $-\infty < t < \infty$.

If x(t) is continuous at $t_0 \in [0, T]$, the series (1-45) converges to the value $x(t_0)$. If x(t) has a jump discontinuity at $t_0 \in [0, T]$, then series (1-45) converges to the midpoint

$$\frac{x(t_0^+) + x(t_0^-)}{2}\,. \tag{1-47}$$

In general, the series (1-45) will not represent x(t) outside of the interval [0, T]. For the special case where x(t) is T-periodic, the series represents x(t) for all t.

The *double-sided amplitude spectrum* of T-periodic x(t) is a plot of $|\zeta_k|$ versus k. The *double-sided phase spectrum* of T-periodic x(t) is a plot of $\measuredangle\zeta_k$ versus k. Usually, phase is defined and plotted in a modulo-2π manner. That is, phase $\measuredangle\zeta_k$ is defined so that

$$\begin{aligned} -\pi < \measuredangle\zeta_k &\le \pi, \quad k > 0 \\ -\pi \le \measuredangle\zeta_k &< \pi, \quad k < 0 \end{aligned} \quad . \tag{1-48}$$

There exists commonly-used terminology for the T-periodic case. ζ_0 is the *DC component*. Frequency ω_0 is the *fundamental frequency*. For k ≥2, $k\omega_0$ is the frequency of the k^th^ harmonic.

Example 1-5: Half-Wave Rectified Sine Wave

Consider the signal

$$\begin{aligned} x(t) &= A\sin(\omega_0 t), \quad 0 \le t \le T/2 \\ &= \quad 0, \quad\quad T/2 \le t \le T \end{aligned} , \tag{1-49}$$

where $\omega_0 = 2\pi/T$, and x(t) = x(t + T). The Fourier series coefficients are

$$\zeta_k = \frac{1}{T}\int_0^{T/2} A\sin(\omega_0 t)e^{-jk\omega_0 t}dt \tag{1-50}$$

For k = 1, this can be computed as

$$\zeta_1 = \frac{1}{T}\int_0^{T/2}\frac{A}{2j}\left[-e^{-j2\omega_0 t}+1\right]dt = \frac{A}{2jT}\left[\frac{e^{-j2\omega_0 t}}{j2\omega_0}+t\right]_{t=0}^{t=T/2} = -j\left(\frac{A}{4}\right) \tag{1-51}$$

For k ≥ 0, k ≠ 1, we can integrate by parts, or use an integral table, to obtain

$$
\begin{aligned}
\zeta_k &= \frac{1}{T}\int_0^{T/2} A\sin(\omega_0 t)e^{-jk\omega_0 t}dt = \frac{A}{T}\frac{e^{-jk\omega_0 t}}{(jk\omega_0)^2+\omega_0^2}\big[-jk\omega_0\sin(\omega_0 t)-\omega_0\cos(\omega_0 t)\big]_{t=0}^{t=T/2} \\
&= \frac{A}{T}\frac{e^{-jk\omega_0 T/2}}{(jk)^2\omega_0+\omega_0}\big[-jk\sin(\omega_0 T/2)-\cos(\omega_0 T/2)\big]-\frac{A}{T}\frac{1}{(jk)^2\omega_0+\omega_0}\big[0-1\big]
\end{aligned} \quad . \tag{1-52}
$$

But, $\omega_0 T = 2\pi$, so that (1-52) becomes

$$
\begin{aligned}
\zeta_k &= A\frac{e^{-jk\pi}}{2\pi(1-k^2)}\big[-jk\sin(\pi)-\cos(\pi)\big]+\frac{A}{2\pi(1-k^2)} = A\frac{(-1)^k+1}{2\pi(1-k^2)} \\
&= \begin{cases} \dfrac{A}{\pi(1-k^2)}, & k \text{ even} \\[2ex] 0, & k \text{ odd}, k \neq 1 \end{cases}
\end{aligned} \quad ,
$$

for $k \geq 0$, $k \neq 1$. Plots of the double-sided amplitude and phase spectrum are depicted by Figure 1-7.

Symmetry Properties of Exponential Fourier Series Coefficients

Indexed on integer k, let ζ_k denote the exponential Fourier series coefficients. If the original function x(t) is real-valued, then it is easy to see that

$$
\zeta_k = \zeta_{-k}^* \tag{1-53}
$$

for all k. Hence, this fact implies the symmetry properties

$$
\begin{aligned}
|\zeta_k| &= |\zeta_{-k}| \\
\measuredangle\zeta_k &= -\measuredangle\zeta_{-k}
\end{aligned} \quad . \tag{1-54}
$$

That is, the magnitude is an even function of index k while the phase is an odd function. Also, it

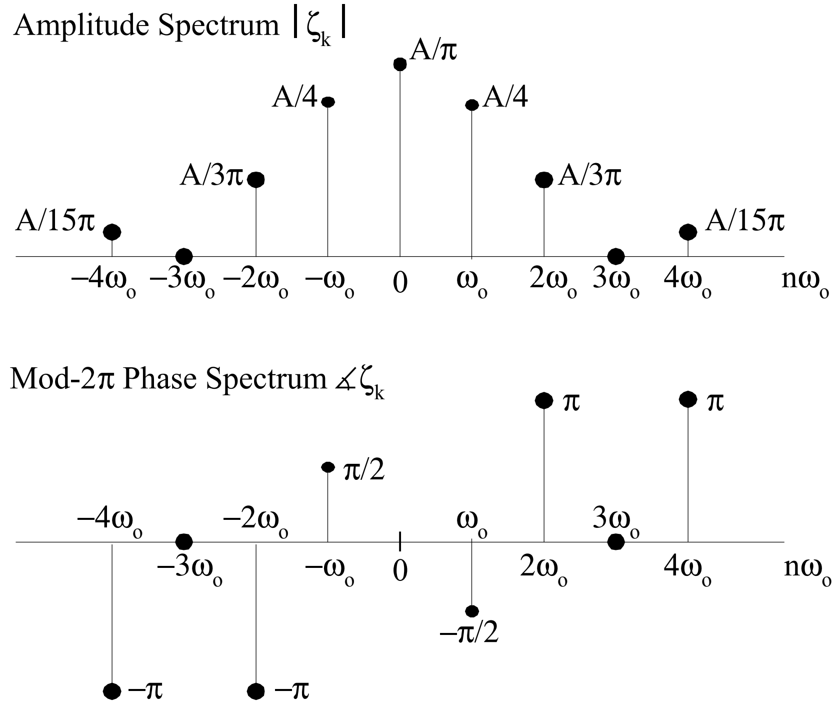

Figure 1-7: Double-sided amplitude and mod-2π phase spectrum of a half-wave rectified sinusoid.

is easily shown that $\mathcal{Re}[\zeta_k]$ is an even function of k, and $\mathcal{Im}[\zeta_k]$ is an odd function.

Parseval's Theorem for Exponential Fourier Series

For the exponential Fourier series, Parseval's theorem says that average power **P** can be expressed as

$$\mathbf{P} = \frac{1}{T}\int_0^T |x(t)|^2\, dt = \sum_{k=-\infty}^{\infty} |\zeta_k|^2 \tag{1-55}$$

Think of Parseval's theorem as giving two ways (using time *and* frequency domain principles) to compute the per-ohm average power of a periodic signal.

Single-Sided Amplitude and Phase Spectra for Real-Valued, Periodic Signals

Suppose x(t) is a real-valued, T-periodic signal. The exponential Fourier series can be written as

$$x(t) = \sum_{k=-\infty}^{\infty} \zeta_k e^{jk\omega_0 t} = \zeta_0 + \sum_{k=1}^{\infty} 2\,\mathrm{Re}\Big[\zeta_k e^{jk\omega_0 t}\Big]$$

$$= \zeta_0 + \sum_{k=1}^{\infty} 2\,\mathrm{Re}\Big[|\zeta_k| e^{j\measuredangle\zeta_k} e^{jk\omega_0 t}\Big] = \zeta_0 + \sum_{k=1}^{\infty} 2|\zeta_k|\,\mathrm{Re}\Big[e^{j(k\omega_0 t + \measuredangle\zeta_k)}\Big] \tag{1-56}$$

$$= \zeta_0 + \sum_{k=1}^{\infty} 2|\zeta_k| \cos(k\omega_0 t + \measuredangle\zeta_k)$$

A plot of ζ_0 at the origin and $2|\zeta_k|$ versus $k\omega_0$, $k > 0$, is known as the *single-sided amplitude spectrum*. A plot of $\measuredangle\zeta_k$ versus $k\omega_0$, $k > 0$, is known as the *single-sided phase spectrum.*

The Fourier Transform

The Fourier series cannot represent an aperiodic function x(t) on the entire time line $-\infty < t < \infty$. In what follows, we seek a frequency domain representation for aperiodic signals. This will lead to the Fourier transform of x(t) which we derive as the formal limit of a Fourier series.

Let x(t) be defined on the entire time line $-\infty < t < \infty$. Use an exponential Fourier series to expand x(t) on the finite interval [-T/2, T/2]; this results in

$$\begin{aligned} x(t) &= \sum_{k=-\infty}^{\infty} \zeta_k e^{jk\omega_0 t}, \quad -T/2 \le t \le T/2 \\ \zeta_k &= \frac{1}{T}\int_{-T/2}^{T/2} x(t) e^{-jk\omega_0 t} dt \end{aligned} \quad , \tag{1-57}$$

where $\omega_0 = 2\pi/T$. Define

$$X(k\omega_0) \equiv T\zeta_k = \int_{-T/2}^{T/2} x(t) e^{-jk\omega_0 t} dt \tag{1-58}$$

so that x(t), $-T/2 \le t \le T/2$, can be represented as

$$x(t) = \frac{1}{2\pi}\sum_{k=-\infty}^{\infty} X(k\omega_0)e^{jk\omega_0 t}\frac{2\pi}{T}, \qquad -T/2 \le t \le T/2. \tag{1-59}$$

Now, consider the *formal* limit of (1-59) as $T \to \infty$, $k\omega_0 \to \omega$ (a new frequency variable), and $(2\pi/T) \to d\omega$. In the limit (1-59) and (1-58) become

$$x(t) = \frac{1}{2\pi}\int_{-\infty}^{\infty} X(\omega)e^{j\omega t}d\omega \tag{1-60}$$

and

$$X(\omega) = \int_{-\infty}^{\infty} x(t)e^{-j\omega t}dt, \tag{1-61}$$

respectively. Transform (1-61) is the *Fourier transform,* and (1-60) is the *inverse Fourier transform*.

Double-Sided Amplitude and Phase Spectra of Fourier Transforms

Often, plots are used to depict a Fourier transform. First, we write the transform in terms of its magnitude and phase as

$$X(\omega) = M(\omega)\exp[j\theta], \tag{1-62}$$

where $M(\omega) = |X(\omega)| = 2\pi A_{dc}\delta(\omega) + M_{ac}(\omega)$, and $\theta(\omega) = \measuredangle X(\omega)$. Here, we use A_{dc} to denote the amplitude of a possible discrete DC component in the wave form, and M_{ac} denotes the AC spectra (*i.e.*, M_{ac} contains no impulse at $\omega = 0$). A plot of $M(\omega)$, $-\infty < \omega < \infty$, is known as a *double-sided amplitude spectrum,* while a plot of $\theta(\omega)$, $-\infty < \omega < \infty$, is known as a *double-sided phase spectrum.* Usually, we plot phase in a *modulo-2π* manner; for $\omega < 0$, define phase so that $-\pi \le \theta < \pi$, and for $\omega > 0$, define phase so that $-\pi < \theta \le \pi$.

Example 1-6: Double-Sided Spectra of a Pulse

Consider the rectangular pulse depicted by Figure 1-8. First, assume that $t_0 = 0$ so that the pulse is symmetrical with respect to the origin. For the case $t_0 = 0$, we can compute

$$X(\omega) = \int_{-\infty}^{\infty} x(t)e^{-j\omega t}dt = 2A\int_0^{\tau/2}\cos(\omega t)dt = \frac{2A}{\omega}\sin(\omega\tau/2) = A\tau\frac{\sin(\omega\tau/2)}{\omega\tau/2}, \qquad (1\text{-}63)$$
$$= A\tau\,\mathrm{Sa}\left(\omega\tau/2\right)$$

where $\mathrm{Sa}(x) \equiv \sin(x)/x$, a standard function in signal processing and communication systems. Now, use the *time-shifting theorem* to compute the Fourier transform of $A\Pi[(t-t_0)/\tau]$ as

$$X(\omega) = A\tau\, e^{-j\omega t_0}\mathrm{Sa}\left(\omega\tau/2\right). \qquad (1\text{-}64)$$

For the case $t_0 = \tau/2$, the double-sided amplitude and phase spectra is depicted by Figure 1-9 (phase is plotted in a modulo-2π manner). For $t_0 = \tau/6$, Figure 1-10 depicts the spectra. Note that the delay value t_0 has a significant effect on the phase function $\theta(\omega)$ (what would the phase plot look like for $t_0 = \tau/4$? For $t_0 = \tau/8$?).

Single-Sided Amplitude and Phase Spectra of the Fourier Transform

If x(t) is real-valued, it is easy to show that $M(\omega) = |X(\omega)|$ and $R(\omega) = \mathcal{Re}[X(\omega)]$ (the real part) are even functions of ω. Likewise, $\theta(\omega) = \measuredangle X(\omega)$ and $I(\omega) = \mathcal{Im}[X(\omega)]$ (the imaginary part) are odd functions. Write $X(\omega) = M(\omega)\exp[j\theta(\omega)] = 2\pi A_{dc}\delta(\omega) + M_{ac}(\omega)\exp[j\theta(\omega)]$. The

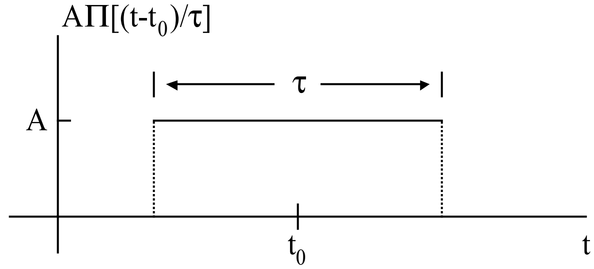

Figure 1-8: $A\Pi[(t-t_0)/\tau]$, a rectangular pulse of width τ which is centered at t_0.

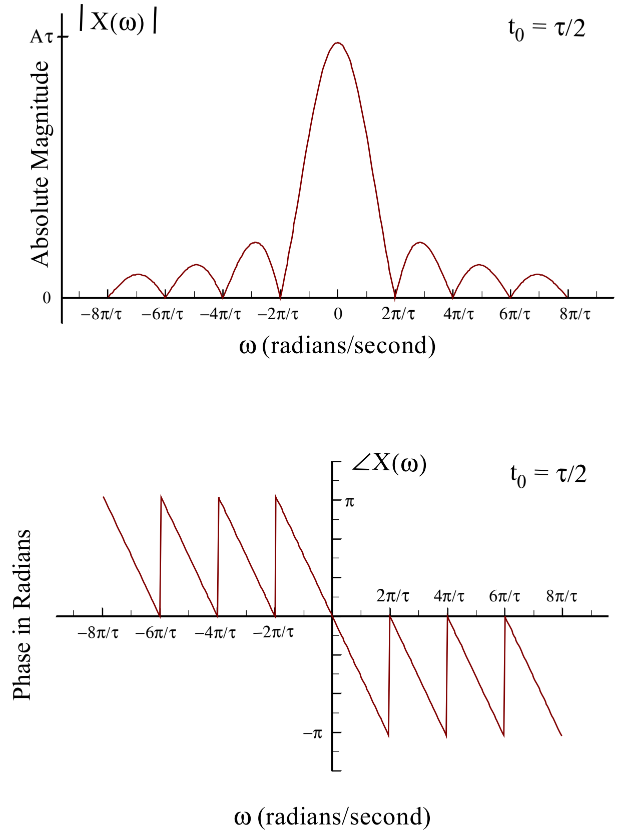

Figure 1-9: Double-sided magnitude and phase spectra for the case $t_0 = \tau/2$.

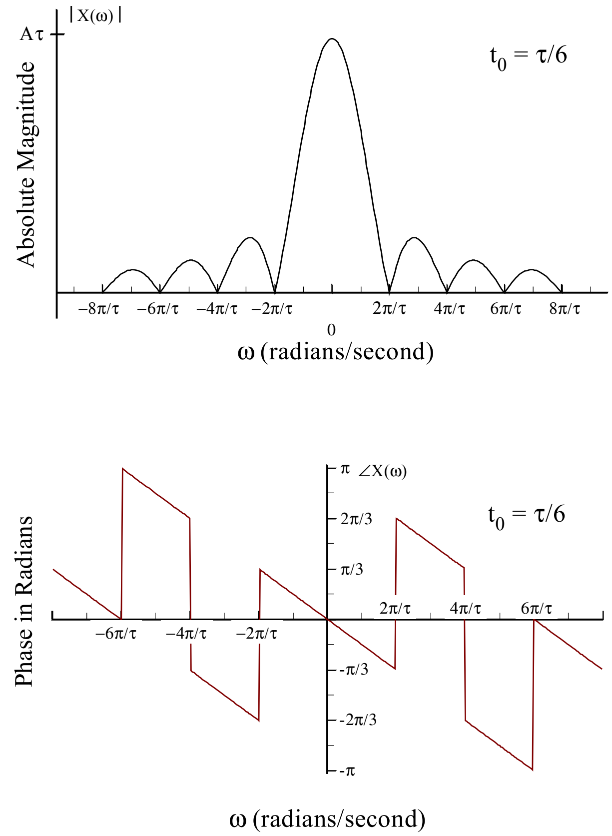

Figure 1-10: Double-sided magnitude and mod-2π phase spectra for the case $t_0 = \tau/6$.

quantity A_{dc} is the DC component (which may be zero) in x(t), and $M_{ac}(\omega)$ contains no impulse at $\omega = 0$. If x(t) is real-valued, we can write

$$\begin{aligned} x(t) &= \frac{1}{2\pi}\int_{-\infty}^{\infty} X(\omega)\, e^{j\omega t} d\omega = \frac{1}{2\pi}\int_{-\infty}^{\infty} [2\pi A_{dc}\delta(\omega) + M_{ac}(\omega) e^{j\theta(\omega)}] e^{j\omega t} d\omega \\ &= A_{dc} + \frac{1}{2\pi}\int_{0}^{\infty} 2M_{ac}(\omega)\cos\{\omega t + \theta(\omega)\}\, d\omega \end{aligned} \quad . \tag{1-65}$$

For $\omega \ge 0$, a plot of $2\pi A_{dc}\delta(\omega) + 2M_{ac}(\omega)$ is known as the *single-sided amplitude spectrum* of the real-valued signal x(t). Likewise, for $\omega \ge 0$, a plot of $\theta(\omega)$ is known as the *single-sided phase spectrum*. No negative frequencies are displayed on the plots. For $\omega > 0$, note the factor of two difference between the single- and double-sided amplitude spectra (both amplitude plots display the same discrete DC component).

Parseval's Theorem for Fourier Transforms of Energy Signals

The energy in an energy signal can be expressed as

$$E = \int_{-\infty}^{\infty} |x(t)|^2 dt = \int_{-\infty}^{\infty} x^*(t)\left[\frac{1}{2\pi}\int_{-\infty}^{\infty} X(\omega)e^{j\omega t}d\omega\right]dt = \int_{-\infty}^{\infty} X(\omega)\left[\frac{1}{2\pi}\int_{-\infty}^{\infty} x^*(t)e^{j\omega t}d\omega\right]dt$$
$$= \frac{1}{2\pi}\int_{-\infty}^{\infty} X(\omega)X^*(\omega)d\omega \quad , (1\text{-}66)$$

which is the same as

$$E = \int_{-\infty}^{\infty} |x(t)|^2 dt = \frac{1}{2\pi}\int_{-\infty}^{\infty} |X(\omega)|^2 d\omega \quad (1\text{-}67)$$

Equation (1-67) is *Parseval's Theorem* for Fourier transforms. Think of this result as providing two methods for calculating the energy in an energy signal. The quantity

$$G(\omega) = |X(\omega)|^2 \quad (1\text{-}68)$$

is called the *energy density spectrum* of energy signal x(t); it has units of Joules/Hz.

Convolution

The convolution of signals f(t) and g(t) is a new function of time. It is defined by

$$f(t) * g(t) \equiv \int_{-\infty}^{\infty} f(\tau)g(t-\tau)d\tau . \quad (1\text{-}69)$$

A simple change of variable produces

$$f(t) * g(t) \equiv \int_{-\infty}^{\infty} f(\tau)g(t-\tau)d\tau = \int_{-\infty}^{\infty} f(t-\tau)g(\tau)d\tau . \quad (1\text{-}70)$$

Hence, you can "fold and shift" f or g in the convolution integral. A close inspection of (1-69) reveals that convolution involves the operations

1) fold $g(\tau)$ to produce $g(-\tau)$,

2) shift $g(-\tau)$ to form $g(t-\tau)$, and

3) integrate the product $f(\tau)g(t-\tau)$ over the range $-\infty < \tau < \infty$.

Example 1-7: Use formula (1-69) to convolve the functions

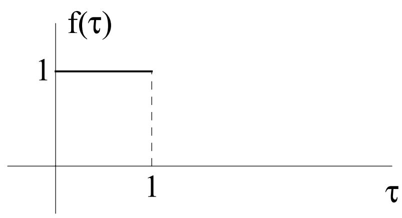

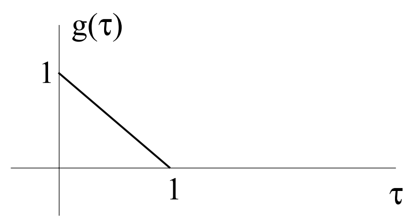

CASE 1: t < 0

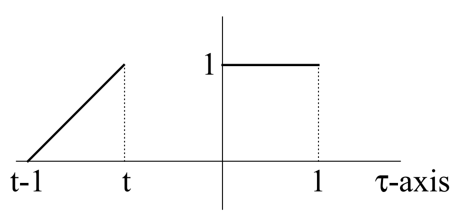

No overlap $\Rightarrow$ $f*g = 0$ for $t < 0$

CASE 2: 0 < t < 1

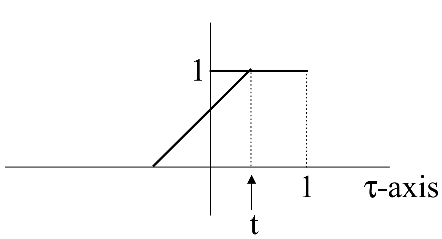

Overlap region from 0 to t

$$\int_0^t 1\cdot(1-[t-\tau])d\tau = \int_0^t (1-t+\tau)d\tau$$

$$= t - t^2/2, \qquad 0 < t < 1$$

CASE 3: 1 < t < 2

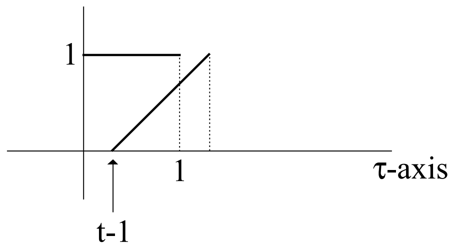

Overlap region from t-1 to 1

$$\int_{t-1}^{1} 1\cdot(1-[t-\tau])d\tau = 2-2t+t^2/2, \quad 1<t<2$$

CASE 4: t > 2

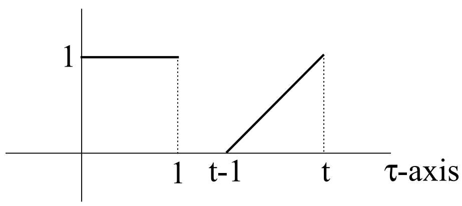

No Overlap

No overlap $\Rightarrow$ f∗g = 0, t > 2

The convolution of f and g is

$$
\begin{aligned}
f*g &= 0, && t<0 \\
&= t-t^2/2, && 0<t<1 \\
&= 2-2t+t^2/2, && 1<t<2 \\
&= 0 && t>2
\end{aligned}
$$

The result of the convolution is depicted by Figure 1-11.

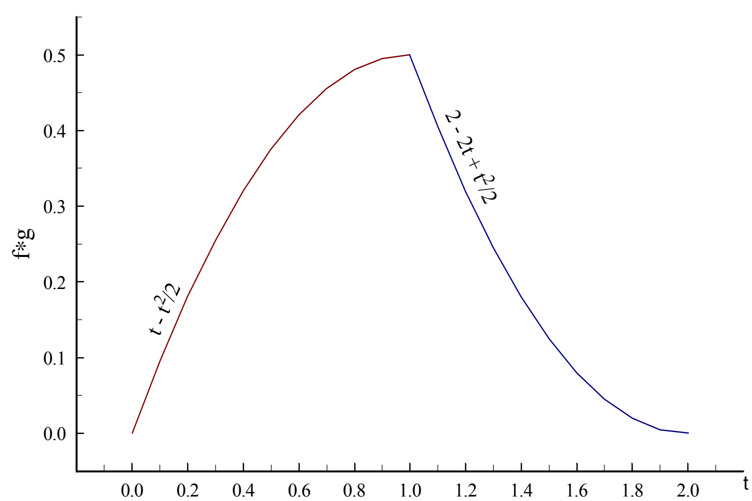

Figure 1-11: Result of the convolution of f and g.

Superposition Theorem

If $x_1(t) \leftrightarrow X_1(\omega)$ and $x_2(t) \leftrightarrow X_2(\omega)$ then, for any constants α and β, we have

$$\alpha x_1(t) + \beta x_2(t) \leftrightarrow \alpha X_1(\omega) + \beta X_2(\omega), \tag{1-71}$$

a result that follows from the fact that integration is a linear operation.

Time Shifting Theorem

If $x(t) \leftrightarrow X(\omega)$, then for any shift t_0, we have

$$x(t - t_0) \leftrightarrow e^{-j\omega t_0} X(\omega). \tag{1-72}$$

Proof:

$$\begin{aligned}\mathfrak{F}[x(t-t_0)] &= \int_{-\infty}^{\infty} x(t-t_0)\, e^{-j\omega t} dt = \int_{-\infty}^{\infty} x(\lambda)\, e^{-j\omega(\lambda+t_0)} d\lambda = e^{-j\omega t_0} \int_{-\infty}^{\infty} x(\lambda)\, e^{-j\omega\lambda} d\lambda \\ &= e^{-j\omega t_0} X(\omega)\end{aligned}. \tag{1-73}$$

Time Scaling Theorem

If $x(t) \leftrightarrow X(\omega)$, then for any non-zero, real-valued constant α, we have

$$x(\alpha t) \leftrightarrow \frac{1}{|\alpha|} X(\omega / \alpha). \tag{1-74}$$

Proof: First assume that $\alpha > 0$ and write

$$\mathfrak{F}[x(\alpha t)] = \int_{-\infty}^{\infty} x(\alpha t)\, e^{-j\omega t} dt = \frac{1}{\alpha}\int_{-\infty}^{\infty} x(\lambda)\, e^{-j(\omega/\alpha)\lambda} d\lambda = \frac{1}{\alpha} X(\omega/\alpha). \tag{1-75}$$

Next, consider the case $\alpha < 0$ and write

$$\begin{aligned}\mathfrak{F}[x(\alpha t)] &= \int_{-\infty}^{\infty} x(\alpha t)\, e^{-j\omega t} dt = \frac{1}{\alpha}\int_{\infty}^{-\infty} x(\lambda)\, e^{-j(\omega/\alpha)\lambda} d\lambda = -\frac{1}{\alpha}\int_{-\infty}^{\infty} x(\lambda)\, e^{-j(\omega/\alpha)\lambda} d\lambda \\ &= -\frac{1}{\alpha} X(\omega/\alpha)\end{aligned} \quad . \tag{1-76}$$

Now, recall the definition

$$\begin{aligned}|\alpha| &= \alpha, \quad \alpha > 0 \\ &= -\alpha, \quad \alpha < 0\end{aligned} \quad . \tag{1-77}$$

Combine the last three equations to obtain (1-74).

Symmetry Theorem

The Fourier transform is symmetrical. That is, x(t) and X(ω) are transform pairs, then we have the *two* pairs

$$\begin{aligned}&x(t) \leftrightarrow X(\omega) \\ &X(t) \leftrightarrow 2\pi\, x(-\omega)\end{aligned} \tag{1-78}$$

Proof: Simply interchange t and ω (after all, *they are just algebraic variables*) in

$$x(t) = \frac{1}{2\pi}\int_{-\infty}^{\infty} X(\omega)\, e^{j\omega t} d\omega$$

to obtain (after multiplication by 2π)

$$2\pi\, x(\omega) = \int_{-\infty}^{\infty} X(t)\, e^{j\omega t} dt \,.$$

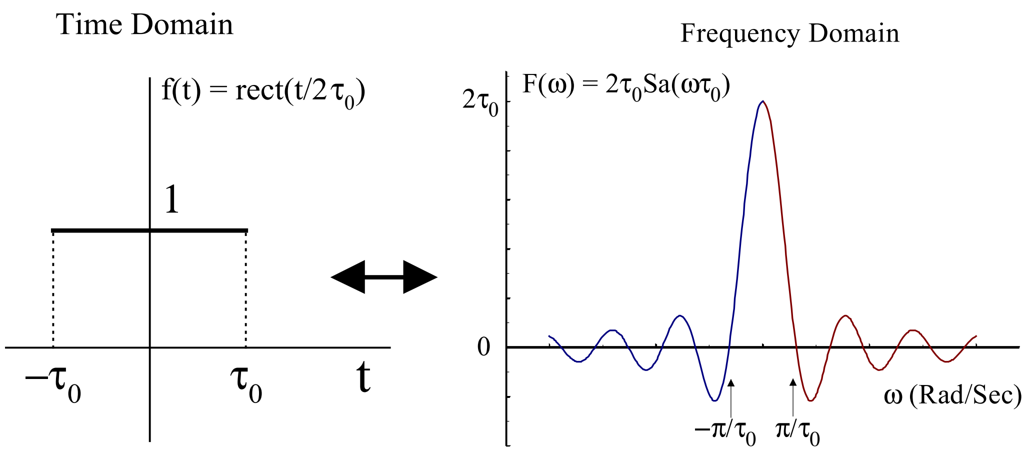

Figure 1-12: Fourier transform found in almost all transform tables.

Now, in this last equation, replace ω by $-\omega$ to obtain

$$2\pi\, x(-\omega) = \int_{-\infty}^{\infty} X(t)\, e^{-j\omega t} dt\,.$$

This last equation is the desired result $X(t) \leftrightarrow 2\pi x(-\omega)$, and this establishes (1-78).

Example 1-8: Suppose we need the Fourier transform of $f(t) = 2\tau_0 Sa(\tau_0 t)$, where $Sa(t) = \sin(t)/t$. We cannot apply the definition directly; the integral is "too hard" to integrate. We cannot find the time-domain function $f(t) = 2\tau_0 Sa(\tau_0 t)$ in our table of Fourier transforms. However, in our table, we do see the transform pair $\mathfrak{F}[rect(t/2\tau_0)] = 2\tau_0 Sa(\omega\tau_0)$, as depicted by Figure 1-12.

Application of the Symmetry Theorem allows us to "flip" this pair and obtain the desired results. So, we conclude that the desired transform is $\mathfrak{F}[2\tau_0 Sa(\tau_0 t)] = 2\pi rect(\omega/2\tau_0)$, as shown by Figure 1-13.

Frequency Shifting Theorem

If $x(t) \leftrightarrow X(\omega)$ then for any frequency shift ω_0 we have

$$x(t)e^{-j\omega_0 t} \leftrightarrow X(\omega + \omega_0) \tag{1-79}$$

Proof: Observe that

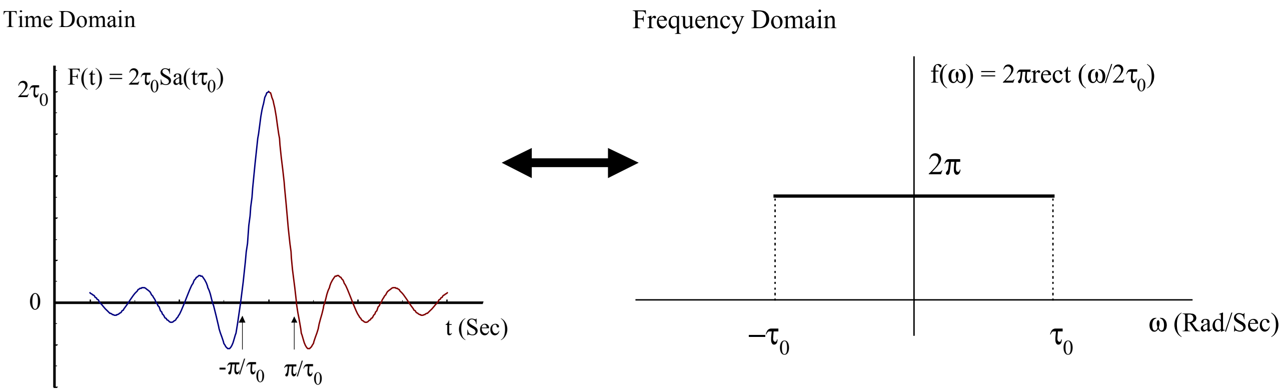

Figure 1-13: Transform pair obtained by applying the symmetry theorem to the pair depicted by Figure 1-12.

$$\mathfrak{F}\left[x(t)e^{-j\omega_0 t}\right] = \int_{-\infty}^{\infty}\{x(t)e^{-j\omega_0 t}\}\, e^{-j\omega t}dt = \int_{-\infty}^{\infty} x(t)e^{-j(\omega_0+\omega)t}dt\,. \tag{1-80}$$

This equation implies

$$x(t)e^{-j\omega_0 t} \leftrightarrow X(\omega+\omega_0)\,, \tag{1-81}$$

the desired result.

Differentiation Theorem

If $x(t) \leftrightarrow X(\omega)$ then

$$\frac{d^n x}{dt^n} \leftrightarrow (j\omega)^n X(\omega) \tag{1-82}$$

Proof

$$\frac{d^n x}{dt^n} = \frac{d^n}{dt^n}\left(\frac{1}{2\pi}\right)\int_{-\infty}^{\infty} X(\omega)e^{j\omega t}d\omega = \frac{1}{2\pi}\int_{-\infty}^{\infty} X(\omega)\frac{d^n}{dt^n}e^{j\omega t}d\omega = \frac{1}{2\pi}\int_{-\infty}^{\infty}\{(j\omega)^n X(\omega)\}e^{j\omega t}d\omega$$

$$= \mathcal{F}^{-1}\left[(j\omega)^n X(\omega)\right]$$

This last result establishes the desired results

$$\frac{d^n x}{dt^n} \leftrightarrow (j\omega)^n X(\omega)\,.$$

Convolution Theorem

Convolution in the time domain gives rise to multiplication in the frequency domain. That is,

$$x_1 * x_2 = \int_{-\infty}^{\infty} x_1(\lambda)x_2(t-\lambda)d\lambda = \int_{-\infty}^{\infty} x_1(t-\lambda)x_2(\lambda)d\lambda \leftrightarrow X_1(\omega)X_2(\omega)\,.$$

Proof

$$\mathcal{F}[x_1 * x_2] = \int_{-\infty}^{\infty} e^{-j\omega t}\left\{\int_{-\infty}^{\infty} x_1(\tau)x_2(t-\tau)d\tau\right\}dt = \int_{-\infty}^{\infty} x_1(\tau)\left\{\int_{-\infty}^{\infty} e^{-j\omega t}x_2(t-\tau)dt\right\}d\tau$$

$$= \int_{-\infty}^{\infty} x_1(\tau)X_2(\omega)e^{-j\omega\tau}d\tau$$

$$= X_1(\omega)X_2(\omega)$$

Integration Theorem

If $x(t) \leftrightarrow X(\omega)$, then

$$\int_{-\infty}^{t} x(\lambda)d\lambda \leftrightarrow \frac{X(\omega)}{j\omega} + \pi X(0)\,\delta(\omega)$$

Proof: Note that the left-hand side of the previous equation can be expressed as

$$\int_{-\infty}^{t} x(\lambda)d\lambda = U(t) * x(t)\,,$$

where U(t) is the unit step function. Use the Convolution Theorem, and take the Fourier transform of this last equation to obtain

$$\begin{aligned}\mathcal{F}\left[\int_{-\infty}^{t} x(\lambda)d\lambda\right] &= \mathcal{F}\left[U(t) * x(t)\right] = \mathcal{F}\left[U(t)\right]\mathcal{F}\left[x(t)\right] = \left[\pi\delta(\omega) + \frac{1}{j\omega}\right]X(\omega) \\ &= \frac{X(\omega)}{j\omega} + \pi\delta(\omega)X(0)\end{aligned} \tag{1-83}$$

Multiplication Theorem

Multiplication in the time domain corresponds to convolution in the frequency domain. That is,

$$x_1(t)x_2(t) \leftrightarrow \frac{1}{2\pi}X_1(\omega) * X_2(\omega) \tag{1-84}$$

Proof: Similar to the Convolution Theorem given above.

Fourier Transform of Periodic Signals

Let x(t) be T-periodic with exponential Fourier series expansion

$$x(t) = \sum_{n=-\infty}^{\infty} \zeta_n e^{jn\omega_0 t},$$

where $\omega_0 = 2\pi/T$. On a term-by-term basis, take the Fourier transform of the series to obtain

$$\mathcal{F}[x(t)] = \sum_{n=-\infty}^{\infty} 2\pi\zeta_n\delta(\omega - n\omega_0), \tag{1-85}$$

a result depicted by Fig 1-14.

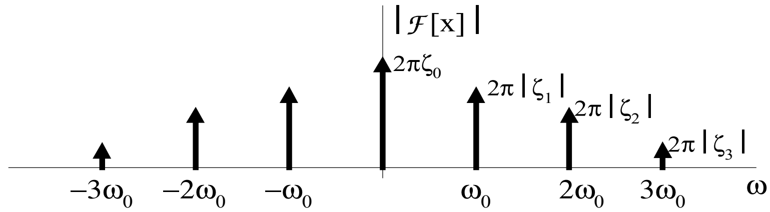

Figure 1-14: Fourier Transform of Periodic Signal

Cross Correlation and Autocorrelation of Energy Signals

Let x(t) and y(t) be complex-valued energy signals. Their *cross correlation* is defined as

$$R_{xy}(\tau) = \int_{-\infty}^{\infty} x^*(t)y(t+\tau)dt\,. \tag{1-86}$$

Crosscorrelation is non-comutative; that is, $R_{xy}(\tau) \neq R_{yx}(\tau)$. However, $R_{xy}(\tau) = R^*_{yx}(-\tau)$ (can you show this result?).

The *autocorrelation* of complex-valued signal x(t) is defined as

$$R_x(\tau) = \int_{-\infty}^{\infty} x^*(t)x(t+\tau)dt \tag{1-87}$$

Note that $R_x(\tau) = R^*_x(-\tau)$ and that

$$R_x(0) = \int_{-\infty}^{\infty} x^*(t)x(t)dt = \int_{-\infty}^{\infty} \left|x(t)\right|^2 dt = \text{Signal Energy}\,. \tag{1-88}$$

An upper bound on $|R_{xy}(\tau)|$ is given by

$$2\left|R_{xy}(\tau)\right| \le R_x(0) + R_y(0)\,. \tag{1-89}$$

We prove this for the case of real-valued signals x and y (the case where x and y are complex-valued is slightly more complicated).

$$\int_{-\infty}^{\infty}[x(u)\pm y(u+\tau)]^2 du = \int_{-\infty}^{\infty} x(u)^2 du + \int_{-\infty}^{\infty} y(u+\tau)^2 du \pm 2\int_{-\infty}^{\infty} x(u)y(u+\tau)du$$
$$= R_x(0) + R_y(0) \pm 2R_{xy}(\tau) \ge 0 \tag{1-90}$$

Hence (1-89) follows as claimed.

If in this last result we use x = y then we have $R_x(0) \ge R_x(\tau)$ for all τ; that is, the maximum autocorrelation occurs at the origin.

Example 1-9:

Calculate the cross correlation $R_{xy}(\tau) = \int_{-\infty}^{\infty} x^*(t)y(t+\tau)dt$ for the two real-valued signals

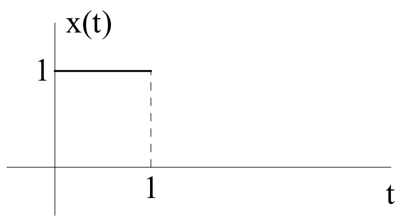

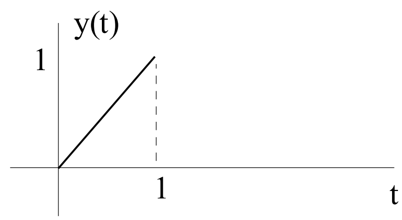

Case 1: $\tau > 1$, no overlap

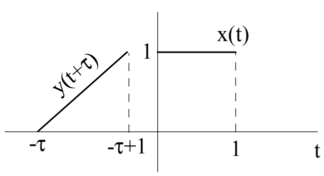

$$R_{xy}(\tau) = 0, \ \tau > 1$$

Case 2: $0 < \tau < 1$

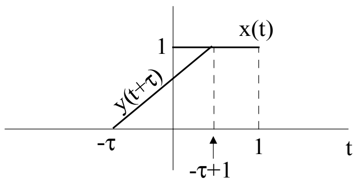

overlap from 0 to -τ+1

$$R_{xy}(\tau) = \int_0^{-\tau+1}(\tau+t)\,dt = -\tfrac{1}{2}[\tau^2-1], \qquad 0 < \tau < 1$$

Case 3: $-1 < \tau < 0$

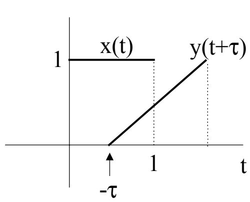

overlap from -τ to 1

$$R_{xy}(\tau) = \int_{-\tau}^{1}(\tau+t)\,dt = \tfrac{1}{2}[\tau+1]^2, \qquad -1 < \tau < 0$$

Case 4: $\tau < -1$

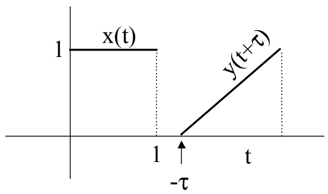

$$R_{xy}(\tau) = 0, \qquad \tau < -1$$

Summary:

$$\begin{aligned} R_{xy}(\tau) &= 0, && ,\tau > 1 \\ &= -\tfrac{1}{2}[\tau^2 - 1] && ,0 < \tau < 1 \\ &= \tfrac{1}{2}[\tau + 1]^2 && ,-1 < \tau < 0 \\ &= 0 && ,\tau < -1 \end{aligned}$$

Relationship between Crosscorrelation and Convolution

Find the relationship between

$$R_{xy}(\tau) = \int_{-\infty}^{\infty} x^*(t)y(t+\tau)dt \quad \text{and} \quad x * y = \int_{-\infty}^{\infty} x(t)y(\tau - t)dt, \tag{1-91}$$

crosscorrelation and convolution, respectively. Use the change of variable v = t + τ in R_{xy} to obtain

$$R_{xy}(\tau) = \int_{-\infty}^{\infty} x^*(v - \tau)y(v)dv = \int_{-\infty}^{\infty} x^*(-[\tau - v])y(v)dv, \tag{1-92}$$

which is just the convolution of x*(-t) and y(t). Hence, $R_{xy}(\tau)$ can be computed by convolving x*(-t) and y(t); that is,

$$R_{xy}(\tau) = x^*(-t) * y(t). \tag{1-93}$$

Fourier Transform of Crosscorrelation - Energy Density Spectrum

Let $x(t) \leftrightarrow X(\omega)$ and $y(t) \leftrightarrow Y(\omega)$ be Fourier transform pairs. From (1-93) and the Convolution Theorem, we obtain

$$\mathcal{F}\left[R_{xy}(\tau)\right] = \mathcal{F}\left[x^*(-t) * y(t)\right] = X^*(\omega)Y(\omega). \tag{1-94}$$

For autocorrelation we have

$$G(\omega) = \mathcal{F}\left[R_x(\tau)\right] = \mathcal{F}\left[x^*(-t) * x(t)\right] = X^*(\omega)X(\omega) = \left|X(\omega)\right|^2, \tag{1-95}$$

the energy density spectrum of energy signal x(t). Hence, *the Fourier transform of the autocorrelation is the energy density spectrum.*

Cross Correlation and Autocorrelation of Power Signals

First, we define a *time averaging* operation as

$$\left\langle z(t)\right\rangle = \underset{T\to\infty}{\text{limit}}\,\frac{1}{2T}\int_{-T}^{T} z(t)\,dt. \tag{1-96}$$

For example, $\langle x^2(t)\rangle$ is the average power in power signal x(t).

Let v(t) and w(t) be power signals. The average $\langle v^*(t)w(t)\rangle$ is called the *scalar product* (or *dot product*) of v(t) and w(t). The scalar product may be complex valued; it serves as a measure of similarity between the two signals.

We define the *cross correlation* of power signals v and w as

$$R_{vw}(\tau) = \left\langle v^*(t)w(t+\tau)\right\rangle = \left\langle v^*(t-\tau)w(t)\right\rangle. \tag{1-97}$$

Note that

$$R_{vw}(\tau) = \left\langle v^*(t)w(t+\tau)\right\rangle = \left\langle v(t)w^*(t+\tau)\right\rangle^* = \left\langle v(t-\tau)w^*(t)\right\rangle^* = \left\langle w^*(t)v(t-\tau)\right\rangle^*, \tag{1-98}$$

and this implies the symmetry condition

$$R_{vw}(\tau) = R^*_{wv}(-\tau), \tag{1-99}$$

a formula identical to that previously obtained for energy signals.

The *autocorrelation* of power signal v(t) is defined as

$$R_v(\tau) = \left\langle v^*(t)v(t+\tau)\right\rangle = \left\langle v^*(t-\tau)v(t)\right\rangle. \tag{1-100}$$

It is possible to show

1) $|R_v(\tau)| \le R_v(0)$ = Avg Pwr {v(t)}, so $|R_v(\tau)|$ has its maximum at $\tau = 0$ (this follows from (1-102)).
2) Since $R^*_v(-\tau) = R_v(\tau)$, if v(t) is real-valued, then $R_v(\tau)$ will be real-valued and even so that $R_v(\tau) = R_v(-\tau)$.
3) If v(t) is T-periodic, then $R_v(\tau)$ is T-periodic.
4) If v(t) **does not** contain discrete frequency sinusoidal components then

$$\underset{\tau\to\infty}{\text{limit}}\, R_v(\tau) = \left|\left\langle v(t)\right\rangle\right|^2 = \text{DC Power in } v(t). \tag{1-101}$$

Given power signals x(t) and y(t), we can show

$$\left|R_{xy}(\tau)\right| \le \frac{1}{2}\left[R_x(0)+R_y(0)\right]. \tag{1-102}$$

This result can be proved in a manner that is identical to that used to establish (1-89) for the energy signal case. Equation (1-102) establishes an upper bound on the cross correlation of two power signals. Note that $|R_{xy}(\tau)|$ may have a maximum for $\tau \neq 0$.

The fact that $R_{vw}(\tau)$ and $R_v(\tau)$ always exists for all τ follows from *Schwarz's Inequality*, a result that is proved below. Schwarz's Inequality states that

$$\left|\left\langle v(t)w^*(t)\right\rangle\right|^2 \le \left\langle |v(t)|^2\right\rangle\left\langle |w(t)|^2\right\rangle \tag{1-103}$$

for any power signals v and w. Now, the right-hand side of this last results is the product of the average powers in the two signals. Since the signals have finite average power, we conclude that $|R_{vw}(\tau)|$, which is the square root of the left-hand side of (1-103), exists (*i.e.,* it is finite).

Schwarz's Inequality

Let P_v and P_w denote the average powers of power signals v(t) and w(t), respectively. Then we have

$$\left|\left\langle v(t)w^*(t)\right\rangle\right|^2 \le \underbrace{\left\langle |v(t)|^2\right\rangle}_{P_v}\ \underbrace{\left\langle |w(t)|^2\right\rangle}_{P_w}. \tag{1-104}$$

(w*(t) can be replaced with w(t) and the inequality still holds).

Proof: Define the power signal

$$z(t) = v(t) - \alpha w(t), \tag{1-105}$$

where α is a to-be-defined complex number. The average power in z(t) is

$$P_z = \left\langle z(t)z^*(t)\right\rangle = \left\langle \{v(t)-\alpha w(t)\}\,\{v^*(t)-\alpha^* w^*(t)\}\right\rangle$$
$$= P_v - 2\,\mathrm{Re}\left[\alpha^*\left\langle v(t)w^*(t)\right\rangle\right] + \alpha\alpha^* P_w \ge 0 \quad , \qquad (1\text{-}106)$$

where we have used $\langle v(t)w^*(t)\rangle = \langle v^*(t)w(t)\rangle^*$. Now, set $\alpha = \langle v(t)w^*(t)\rangle / P_w$ and obtain

$$P_z = P_v - 2\,\mathrm{Re}\left[\frac{\left|\left\langle v(t)w^*(t)\right\rangle\right|^2}{P_w}\right] + \frac{\left|\left\langle v(t)w^*(t)\right\rangle\right|^2}{P_w^2}P_w \ge 0$$
$$= P_v - \frac{\left|\left\langle v(t)w^*(t)\right\rangle\right|^2}{P_w} \ge 0 \qquad (1\text{-}107)$$

from which the desired results (1-104) follows.

Equality in (1-104) holds if, and only if, v(t) is proportional to w(t); that is, equality in (1-104) holds iff v(t) = kw(t) for some constant k.

Uncorrelated Signals

Two signals v(t) and w(t) are said to be *uncorrelated* if $R_{vw}(\tau) = 0$ for all τ. Let v(t) and w(t) be uncorrelated and form the sum z(t) = v(t) + w(t). Then

$$R_z(\tau) = \left\langle \{v(t)+w(t)\}\,\{v^*(t)+w^*(t)\}\right\rangle = \left\langle v(t)v^*(t)\right\rangle + \left\langle w(t)w^*(t)\right\rangle$$
$$= R_v(\tau) + R_w(\tau) \qquad (1\text{-}108)$$

so autocorrelations add. Hence, for uncorrelated signal, the power of the sum is the sum of the powers (power obeys superposition for uncorrelated signals: $P_{V+W} = P_V + P_W$).

Crosscorrelation of T-periodic Power Signals in Terms of Fourier Series

If x(t) and y(t) are periodic with period T_0, then cross correlation $R_{xy}(\tau)$ is periodic with period T_0. Furthermore, to calculate the cross correlation, you only need integrate over one period of the waveforms. That is, for T_0-periodic x(t) and y(t), we can compute

$$R_{xy}(\tau) = \frac{1}{T_0}\int_0^{T_0} x^*(t)y(t+\tau)\,dt\,. \tag{1-109}$$

For the periodic case just considered, we can express the Fourier series of $R_{xy}(\tau)$ in terms of the Fourier series of x and y. Express T_0-periodic x and y as

$$\begin{aligned} x(t) &= \sum_{k=-\infty}^{\infty} \alpha_k\, e^{jk\omega_0 t} \\ &\qquad\qquad\qquad , \\ y(t) &= \sum_{k=-\infty}^{\infty} \beta_k\, e^{jk\omega_0 t} \end{aligned} \tag{1-110}$$

where $\omega_0 = 2\pi/T_0$ is the fundamental frequency of the signals. Then, we can write

$$\begin{aligned} R_{xy}(\tau) &= \frac{1}{T_0}\int_0^{T_0} x^*(t)y(t+\tau)\,dt = \frac{1}{T_0}\int_0^{T_0}\left(\sum_{n=-\infty}^{\infty}\alpha_n^*\, e^{-jn\omega_0 t}\right)\left(\sum_{m=-\infty}^{\infty}\beta_m\, e^{jm\omega_0 t}e^{jm\omega_0\tau}\right)dt \\ &= \sum_{n=-\infty}^{\infty}\sum_{m=-\infty}^{\infty}\alpha_n^*\,\beta_m e^{jm\omega_0\tau}\frac{1}{T_0}\int_0^{T_0} e^{j(m-n)\omega_0 t}dt \end{aligned} \tag{1-111}$$

Now, the complex exponential functions are orthogonal so that

$$\begin{aligned} \frac{1}{T_0}\int_0^{T_0} e^{j(m-n)\omega_0 t}dt &= 1, \quad n = m \\ & \qquad\qquad , \\ &= 0, \quad n \neq m \end{aligned} \tag{1-112}$$

and this fact leads to the simple formula

$$R_{xy}(\tau) = \sum_{n=-\infty}^{\infty} \alpha_n^* \beta_n e^{jn\omega_0\tau} \tag{1-113}$$

for the T_0-periodic cross correlation. Similarly, T_0-periodic x(t) has a T_0-periodic autocorrelation given by

$$R_x(\tau) = \sum_{n=-\infty}^{\infty} |\alpha_n|^2 \, e^{jn\omega_0\tau}\,. \tag{1-114}$$

Power Spectral Density

We are interested in defining the *power spectrum* $\boldsymbol{S}(\omega)$ of power signal x(t). The power spectrum should be a real-valued, nonnegative function. It should be an even function of ω if x(t) is real-valued. Furthermore, the total average power should be obtained by integrating $\boldsymbol{S}(\omega)/2\pi$ over all frequency, that is, the total average per-ohm power should be obtained from

$$P_{avg} = \operatorname*{limit}_{T\to\infty} \frac{1}{2T}\int_{-T}^{T} |x(t)|^2\, dt = \frac{1}{2\pi}\int_{-\infty}^{\infty} \boldsymbol{S}(\omega)d\omega \qquad \text{(watts)}\,. \tag{1-115}$$

From (1-115), it is easily seen that the units associated with $\boldsymbol{S}(\omega)$ are watts/Hz.

Example 1-10: Consider a T-periodic power signal x(t). In a Fourier series, expand x(t) as

$$x(t) = \sum_{n=-\infty}^{\infty} \zeta_n e^{jn\omega_0 t}\,. \tag{1-116}$$

The power spectrum of the T-periodic signal is

$$\boldsymbol{S}(\omega) = \sum_{n=-\infty}^{\infty} 2\pi|\zeta_n|^2\, \delta(\omega - n\omega_0)\,. \tag{1-117}$$

This follows since

$$\frac{1}{2\pi}\int_{-\infty}^{\infty} \boldsymbol{S}(\omega)d\omega = \frac{1}{2\pi}\int_{-\infty}^{\infty} \sum_{n=-\infty}^{\infty} 2\pi|\zeta_n|^2 \delta(\omega - n\omega_0)d\omega = \sum_{n=-\infty}^{\infty} |\zeta_n|^2 = P_{avg} \tag{1-118}$$

by Parseval's Theorem.

We seek a general method to represent/compute the power spectrum. Towards this end, consider *windowing* power signal x(t) to form

$$x_T(t) \equiv x(t)\text{rect}(t/T), \tag{1-119}$$

where

$$\begin{aligned} \text{rect(t/T)} &= 1, \quad -T/2 < t < T/2 \\ &= 0, \qquad \text{otherwise} \end{aligned} \tag{1-120}$$

is a T-long time window centered at the origin. Windowed signal x_T is an energy signal, and its Fourier transform is denoted by

$$\mathbf{X}_T(\omega) \equiv \mathcal{F}\left[x(t)\text{rect}(t/T)\right]. \tag{1-121}$$

By Parseval's theorem for Fourier transforms, we have

$$\int_{-T/2}^{T/2} |x_T(t)|^2\, dt = \frac{1}{2\pi}\int_{-\infty}^{\infty} |\mathbf{X}_T(\omega)|^2\, d\omega \tag{1-122}$$

for all T. Hence, the average power is given by

$$\lim_{T\to\infty}\frac{1}{T}\int_{-T/2}^{T/2}\left|x_T(t)\right|^2 dt = \lim_{T\to\infty}\frac{1}{T}\left[\frac{1}{2\pi}\int_{-\infty}^{\infty}\left|\mathbf{X}_T(\omega)\right|^2 d\omega\right] = \frac{1}{2\pi}\int_{-\infty}^{\infty}\lim_{T\to\infty}\frac{\left|\mathbf{X}_T(\omega)\right|^2}{T}d\omega . \qquad (1\text{-}123)$$

Hence, from (1-115) and (1-123) we see that

$$\frac{1}{2\pi}\int_{-\infty}^{\infty}\boldsymbol{S}(\omega)d\omega = \frac{1}{2\pi}\int_{-\infty}^{\infty}\lim_{T\to\infty}\frac{\left|\mathbf{X}_T(\omega)\right|^2}{T}d\omega . \qquad (1\text{-}124)$$

As part of our definition of $\boldsymbol{S}$, we require that (1-124) hold over arbitrary frequency bands (frequency intervals). This requirement leads to

$$\frac{1}{2\pi}\int_{-\infty}^{\omega}\boldsymbol{S}(\rho)d\rho = \frac{1}{2\pi}\int_{-\infty}^{\omega}\lim_{T\to\infty}\frac{\left|\mathbf{X}_T(\rho)\right|^2}{T}d\rho \qquad (1\text{-}125)$$

for all values of ω. Basically, we get the power that is contained in the (ω_1, ω_2) frequency band if we integrate $\boldsymbol{S}(\omega)/2\pi$ over this band.

Now, we can write a general formula for the power spectrum. With respect to frequency, differentiate (1-125) to obtain

$$\boldsymbol{S}(\omega) \equiv \lim_{T\to\infty}\frac{\left|\mathbf{X}_T(\omega)\right|^2}{T}, \qquad (1\text{-}126)$$

an important formula for the power spectrum.

Equation (1-126) suggests a practical way to approximate the power spectrum of a power signal. First, a data record of length T is recorded. Next, the Fourier transform $\mathbf{X}_T(\omega)$ of the time record $x_T(t)$ is computed/approximated (often, by an FFT). Finally, the power spectrum is approximated by $|\mathbf{X}_T(\omega)|^2/T$, a result that may be plotted as a function of frequency ω.

Example 1-11: Use (1-126) with a large value of T to approximate the power spectrum of power signal A$\exp(j\omega_0 t)$. How does the approximation behave as T approaches infinity? First, consider the windowed signal x_T = A$\exp(j\omega_0 t)$rect(t/T) with transform

$$\mathbf{X}_T(\omega) \equiv \mathcal{F}\left[\mathrm{A}\exp(j\omega_0 t)\mathrm{rect}(t/T)\right] = \mathrm{AT}\,\mathrm{Sa}\left[(\omega-\omega_0)\mathrm{T}/2\right] \tag{1-127}$$

so that for large, finite T we have

$$\boldsymbol{S}(\omega) \approx \frac{\left|\mathbf{X}_T(\omega)\right|^2}{\mathrm{T}} = \mathrm{A}^2\mathrm{T}\left[\mathrm{Sa}\left[(\omega-\omega_0)\mathrm{T}/2\right]\right]^2 \tag{1-128}$$

as our approximation to the power spectrum. This approximation is illustrated by Figure 1-15; note that the base width is proportional to $4\pi/T$ and the height is proportional to A^2T. In the limit as $T \to \infty$, this last equation produces

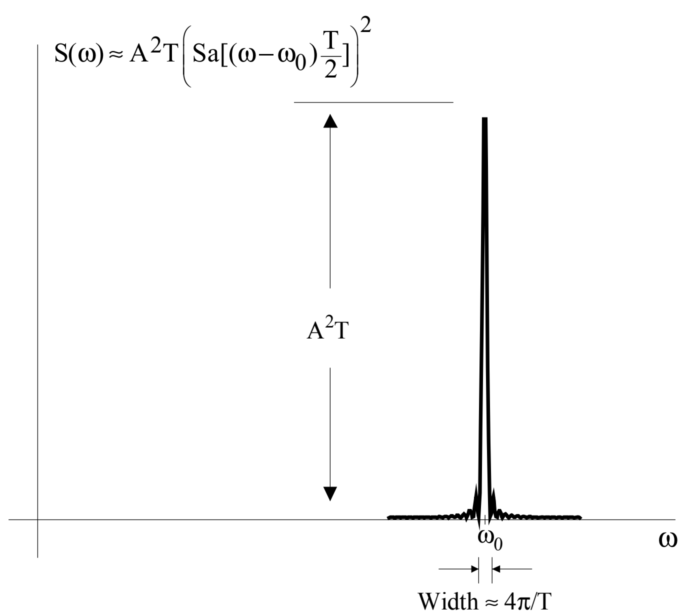

Figure 1-15: Approximation to power spectrum. The approximation approaches $2\pi A^2\delta(\omega-\omega_0)$ as $T \to \infty$.

$$\boldsymbol{S}(\omega) = \underset{T\to\infty}{\text{limit}} \frac{|\mathbf{X}_T(\omega)|^2}{T} = A^2 \underset{T\to\infty}{\text{limit}}\, T\left[\text{Sa}\left[(\omega-\omega_0)T/2\right]\right]^2$$
$$= 2\pi A^2 \underset{T\to\infty}{\text{limit}} \frac{T}{2\pi}\text{Sa}^2\left[(\omega-\omega_0)T/2\right] = 2\pi A^2\delta(\omega-\omega_0) \tag{1-129}$$

as the power spectrum.

System Input - Output Cross Correlation and Output Autocorrelation

Let x(t) and y(t) denote the input and output, respectively, of a linear, time-invariant system having h(t) as its impulse response. We show that $R_{xy}(t) = h(t)*R_x(t)$ for the case where x and y are energy signals; the result is true for power signals as well. Let x and y be energy signals and observe

$$R_{xy}(\tau) = \int_{-\infty}^{\infty} x^*(t)y(t+\tau)dt = \int_{-\infty}^{\infty} x^*(t)\left[\int_{-\infty}^{\infty} h(u)x(t+\tau-u)du\right]dt$$
$$= \int_{-\infty}^{\infty} h(u)\left[\int_{-\infty}^{\infty} x^*(t)x(t+\tau-u)dt\right]du \tag{1-130}$$
$$= \int_{-\infty}^{\infty} h(u)R_x(\tau-u)du\,.$$

Hence, it follows that $R_{xy}(\tau) = h(\tau)*R_x(\tau)$ as claimed. As stated previously, this result holds for power signals as well as energy signals.

It is possible to compute the output autocorrelation from knowledge of the input autocorrelation and the system's impulse response. To see how this is done, consider

$$R_y(\tau) = \int_{-\infty}^{\infty} y^*(t)y(t+\tau)dt = \int_{-\infty}^{\infty}\left[\int_{-\infty}^{\infty} h^*(u)x^*(t-u)du\right]y(t+\tau)dt$$
$$= \int_{-\infty}^{\infty} h^*(u)\left[\int_{-\infty}^{\infty} x^*(t-u)y(t+\tau)dt\right]du\,. \tag{1-131}$$

In this result replace the t variable with $v \equiv t - u$ to obtain

$$
\begin{aligned}
R_y(\tau) &= \int_{-\infty}^{\infty} h^*(u)\left[\int_{-\infty}^{\infty} x^*(v)y(v+u+\tau)dv\right]du \\
&= \int_{-\infty}^{\infty} h^*(u)R_{xy}(u+\tau)du \qquad (1\text{-}132) \\
&= \int_{-\infty}^{\infty} h^*(-u)R_{xy}(\tau-u)du,
\end{aligned}
$$

the convolution of $h^*(-\tau)$ and $R_{XY}(\tau)$. Now, from the previous page we have

$$
\begin{aligned}
R_y(t) &= R_{xy}(t) * h(-t) = \left[h(t) * R_x(t)\right] * h(-t) \\
&= \left[h(t) * h(-t)\right] * R_x(t), \qquad (1\text{-}133)
\end{aligned}
$$

so that the autocorrelation of the output can be expressed as the autocorrelation of the input convolved with $h(\tau)*h^*(-\tau)$.

Power Spectrum as Fourier Transform of Autocorrelation - *The Wiener-Khinchine Theorem*

Recall that the power spectrum of power signal x(t) is

$$
\boldsymbol{S}(\omega) = \underset{T\to\infty}{\text{limit}} \frac{\left|X_T(\omega)\right|^2}{T}. \qquad (1\text{-}134)
$$

Take the inverse Fourier transform of $\boldsymbol{S}$ to obtain

$$\mathcal{F}^{-1}[\boldsymbol{S}(\omega)] = \frac{1}{2\pi}\int_{-\infty}^{\infty} \underset{T\to\infty}{\text{limit}} \frac{|X_T(\omega)|^2}{T} e^{j\omega\tau} d\omega$$

$$= \underset{T\to\infty}{\text{limit}} \frac{1}{2\pi}\int_{-\infty}^{\infty} \frac{1}{T}\Big[\int_{-T/2}^{T/2} x^*(t_1)e^{j\omega t_1}dt_1\Big]\Big[\int_{-T/2}^{T/2} x(t_2)e^{-j\omega t_2}dt_2\Big]e^{j\omega\tau}d\omega. \tag{1-135}$$

$$= \underset{T\to\infty}{\text{limit}} \frac{1}{T}\int_{-T/2}^{T/2} x^*(t_1)\int_{-T/2}^{T/2} x(t_2)\Big[\frac{1}{2\pi}\int_{-\infty}^{\infty} e^{j\omega(t_1-t_2+\tau)}d\omega\Big]dt_2 dt_1$$

However, from Fourier transform theory we know that

$$\frac{1}{2\pi}\int_{-\infty}^{\infty} e^{j\omega(t_1-t_2+\tau)}d\omega = \delta(t_1 - t_2 + \tau). \tag{1-136}$$

Now, use (1-136) in (1-135) to obtain

$$\mathcal{F}^{-1}[\boldsymbol{S}(\omega)] = \underset{T\to\infty}{\text{limit}} \frac{1}{T}\int_{-T/2}^{T/2} x^*(t_1)\int_{-T/2}^{T/2} x(t_2)\delta(t_1 - t_2 + \tau)dt_2 dt_1$$

$$= \underset{T\to\infty}{\text{limit}} \frac{1}{T}\int_{-T/2}^{T/2} x^*(t)x(t+\tau)dt = \Big\langle x^*(t)x(t+\tau)\Big\rangle .$$

$$= R_x(\tau)$$

This is the well-known, and very useful, *Wiener-Khinchine Theorem*: the Fourier transform of the autocorrelation is the power spectrum density. Symbolically, we write

$$R_x(\tau) \longleftrightarrow \boldsymbol{S}(\omega). \tag{1-137}$$

Power Signals in Systems: Input/Output of Power Spectrums

Suppose power signal x(t) is input to a linear, time-invariant system to produce y(t), the output power signal. How can we find the output power spectrum in terms of the input power spectrum? By the Wiener-Kinchine theorem, we can write the power spectrum of output y(t) as

$$\boldsymbol{S}_y(\omega) = \mathcal{F}\left[R_y(\tau)\right]. \tag{1-138}$$

Use the fact that $R_y(\tau) = [h(t)*h^*(-t)]*R_x(\tau)$ to write

$$\boldsymbol{S}_y(\omega) = \mathcal{F}\left[R_y(\tau)\right] = \mathcal{F}\left[\left(h(t)*h^*(-t)\right)*R_x(\tau)\right] = \mathcal{F}\left[h(t)*h^*(-t)\right]\mathcal{F}\left[R_x(\tau)\right]. \tag{1-139}$$

However, $\mathcal{F}[h^*(-t)] = H^*(j\omega)$ so that

$$\begin{aligned}\boldsymbol{S}_y(\omega) &= \mathcal{F}\left[h(t)*h^*(-t)\right]\mathcal{F}\left[R_x(\tau)\right] = H^*(j\omega)H(j\omega)\,\boldsymbol{S}_x(\omega) \\ &= \left|H(j\omega)\right|^2 \boldsymbol{S}_x(\omega)\end{aligned}, \tag{1-140}$$

an important result that is used in many applications in signal processing, radar, etc (see Fig. 1-16).

Periodic Signals

Let x(t) be T-periodic with Fourier series expansion

$$x(t) = \sum_{k=-\infty}^{\infty} \alpha_k\, e^{jk\omega_0 t}\,, \tag{1-141}$$

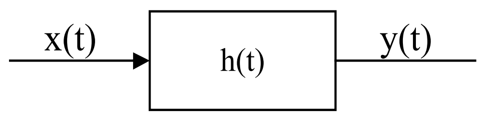

Input Power Spectrum $\boldsymbol{S}_x(\omega)$ Output Power Spectrum $\boldsymbol{S}_y(\omega)$

Figure 1-16: Linear system. Output spectrum is related to input spectrum by $\boldsymbol{S}_y(\omega) = |H(j\omega)|^2 \boldsymbol{S}_x(\omega)$.

where $\omega_0 = 2\pi/T$. Recall from (1-114) that the autocorrelation of x is

$$R_x(\tau) = \sum_{n=-\infty}^{\infty} |\alpha_n|^2 \; e^{jn\omega_0\tau}\,. \tag{1-142}$$

From the Wiener-Kinchine Theorem we have the power spectrum as

$$\boldsymbol{S}(\omega) = \mathcal{F}\left[R_x(\tau)\right] = \sum_{n=-\infty}^{\infty} |\alpha_n|^2 \mathcal{F}\left[e^{jn\omega_0\tau}\right] = 2\pi \sum_{n=-\infty}^{\infty} |\alpha_n|^2 \delta(\omega - n\omega_0)\,. \tag{1-143}$$

Note that all of the power is concentrated at DC and the various discrete frequency components in the signal.

Signals and Systems

A *system* is a mapping between an input x(t) and an output y(t). Notice that our system, depicted by Fig. 1-17, has a single input and a single output. It is possible to generalize this concept to systems with multiple inputs and outputs.

Linearity

The system is said to be *linear* if it obeys superposition. Let x_1 and x_2 be arbitrary inputs; assume that x_1 and x_2 produce outputs y_1 and y_2, respectively. Then the system is said to *linear* if, for any constants α and β, the input $\alpha x_1 + \beta x_2$ produces the output $\alpha y_1 + \beta y_2$.

Let $h(t,\tau)$ denote the system's response at time t to an δ function applied at time τ, an input/output relationship depicted by Fig. 1-18. Function $h(t,\tau)$ is called the system's *impulse response*. It is well-known that the system's output y(t) is given by

Figure 1-17: A system with input x(t) and output y(t).

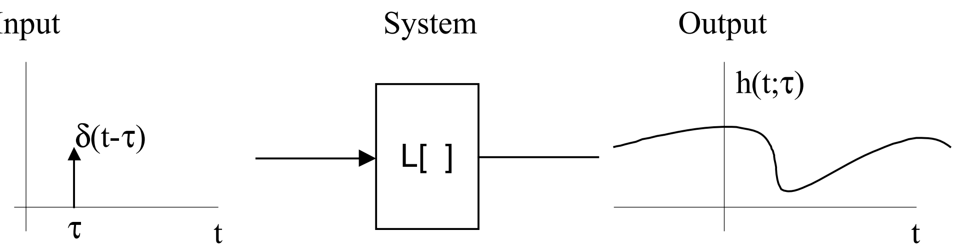

Figure 1-18: An impulse applied at time τ produces h(t,τ) at time t.

$$y(t) = \int_{-\infty}^{\infty} h(t,\tau)x(\tau)d\tau, \qquad -\infty < t < \infty. \tag{1-140}$$

As discussed below, this input-output (I/O) relationship can take on various forms depending on the system properties of time invariance and causality.

Time Invariance

Let x(t) and y(t) be an arbitrary input/output pair. The system is said to be *time invariant* if input $x(t - t_0)$ produces output $y(t - t_0)$ for any time shift t_0. This idea is conveyed by Figure 1-19. For a time-invariant system, the output at time t to an input applied at time τ depends on the *time difference* t - τ and **not** on the absolute value of t or τ. For this reason, h(t, τ) = h(t - τ), and

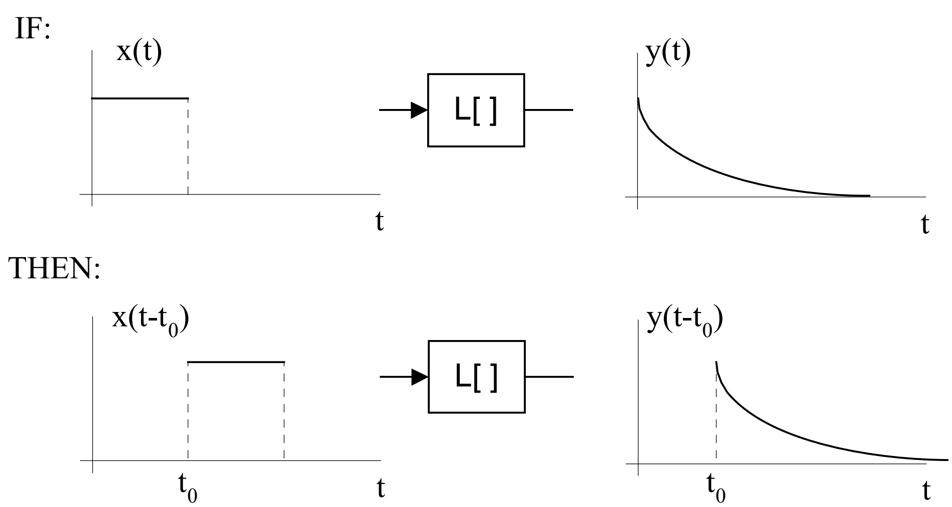

Figure 1-19: Time-invariance: if y(t) = L[x(t)] are any input-output pair, then $y(t-t_0) = L[x(t-t_0)]$ for any t_0.

the input-output relationship (1-140) becomes

$$y(t) = \int_{-\infty}^{\infty} h(t-\tau)x(\tau)d\tau, \qquad -\infty < t < \infty, \tag{1-141}$$

since the impulse response depends on the time difference and not absolute t or τ. Equation (1-141) states that output y(t) is the *convolution* of input x(t) and impulse response h(t).

Causality

Let $x_1(t)$ and $x_2(t)$ be arbitrary inputs which produce outputs $y_1(t)$ and $y_2(t)$, respectively. The system is said to be *causal* if $x_1(t) = x_2(t)$, $t < t_0$, for any t_0, implies that $y_1(t) = y_2(t)$ for $t < t_0$. Note that $x_1(t)$, $x_2(t)$ and t_0 are not system dependent (they are arbitrary except for the requirement that $x_1(t) = x_2(t)$, $t < t_0$ for some t_0). Basically, a causal system cannot respond before it is excited; its output y at time t does not depend on input x at time greater than t.

One can show that a *linear, time-invariant system is causal if, and only if, its impulse response* h(t) *vanishes for* t < 0. That is, a necessary and sufficient condition for causality is

$$h(t) = 0, \qquad t < 0. \tag{1-142}$$

For linear, time-invariant causal systems, relationship (1-141) becomes

$$y(t) = \int_{-\infty}^{t} h(t-\tau)x(\tau)d\tau, \qquad -\infty < t < \infty, \tag{1-143}$$

where it is assumed that input x(t) starts (was initially applied) in the infinite past.

Bounded Input - Bounded Output Stability (BIBO Stability)

A linear system is said to be *bounded input - bounded output stable* (BIBO stable) if bounded inputs always produce bounded outputs. It can be shown that a linear, time-invariant system is BIBO stable if, and only if,

$$\int_{-\infty}^{\infty} |h(t)| dt < \infty . \tag{1-144}$$

That is, the system is BIBO stable if, and only if, h(t) is absolutely integrable.

Transfer Function

Linear, time-invariant systems can be described in the frequency domain by using the Fourier transform. Take the Fourier transform of (1-141) to obtain

$$Y(\omega) = H(\omega)X(\omega) , \tag{1-145}$$

where Y, H and X are Fourier transforms of y, h and x, respectively. $H(\omega)$ is called the *transfer function* of the system. If h(t) is real-valued, then $\mathrm{Re}[H(\omega)]$ is even and $\mathrm{Im}[H(\omega)]$ is odd (so that $|H(\omega)|$ is even and $\measuredangle H(\omega)$ is odd). A plot of $|H(\omega)|$ is called the *double-sided amplitude response*, and a plot of $\measuredangle H(\omega)$ is called the *double-sided phase response*.

Example 1-12: Consider the circuit depicted by Figure 1-20. A relationship between input x and output y is given by

$$RC\frac{dy}{dt} + y = x . \tag{1-146}$$

From elementary ordinary differential equation theory, the *complete* solution of (1-146) is given by

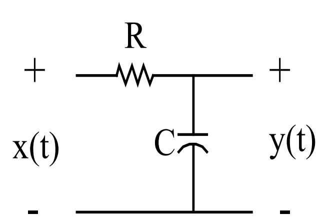

Figure 1-20: A simple first-order system

$$y(t) = e^{-(t-t_0)/\tau_0}\left[\frac{1}{\tau_0}\int_{t_0}^{t} e^{(\lambda-t_0)/\tau_0}x(\lambda)\,d\lambda + y(t_0)\right], \qquad t \ge t_0, \tag{1-147}$$

where τ_0 = RC is the circuit time constant, and $y(t_0)$ is the initial voltage across the capacitor at t = t_0.

Assume that all initial conditions are zero. From (1-147), the output for $t \ge 0$ is given by

$$y(t) = \int_0^t h(t-\lambda)x(\lambda)\,d\lambda, \qquad t \ge 0, \tag{1-148}$$

where

$$h(t) = \frac{1}{\tau_0}e^{-t/\tau_0}U(t) \tag{1-149}$$

is the circuit impulse response.

The transfer function of this system is given by

$$H(\omega) = \mathscr{F}[h(t)] = \frac{1}{1 + j\omega/\omega_0}, \tag{1-150}$$

where ω_0 = 1/RC is the 3dB cut off frequency of the filter.

Periodic Response to Periodic Input

A T-periodic response can be obtained from a linear, time-invariant system that is driven by a T-periodic forcing function. Let the input x(t) be represented as

$$x(t) = \sum_{n=-\infty}^{\infty} c_n e^{jn\omega_0 t}. \tag{1-151}$$

Let the system impulse response be h(t) so that the output can be computed as

$$y(t) = \int_{-\infty}^{\infty}\left[\sum_{n=-\infty}^{\infty} c_n e^{jn\omega_0(t-\tau)}\right]h(\tau)d\tau = \sum_{n=-\infty}^{\infty}\left[\int_{-\infty}^{\infty} e^{-jn\omega_0\tau}h(\tau)d\tau\right]c_n e^{jn\omega_0 t}$$
$$= \sum_{n=-\infty}^{\infty} H(n\omega_0)c_n e^{jn\omega_0 t} \qquad (1\text{-}152)$$

where $H(\omega) = \mathcal{F}[h(t)]$, the Fourier transform of the impulse response (*i.e.*, the transfer function). Note that $c_nH(n\omega_0)$, $-\infty < n < \infty$, are the Fourier series coefficients of the periodic output.

For the simple case where $x(t) = A\cos(\omega_0 t)$, the output is

$$y(t) = \frac{A}{2}\left[H(\omega_0)e^{j\omega_0 t} + H(-\omega_0)e^{-j\omega_0 t}\right] = A\,\mathrm{Re}\left[\left|H(\omega_0)\right|e^{j\{\omega_0 t + \measuredangle H(\omega_0)\}}\right]$$
$$= A\left|H(\omega_0)\right|\cos\{\omega_0 t + \measuredangle H(\omega_0)\}. \qquad (1\text{-}153)$$

Piecewise Description of Periodic Response

Often, with simple first- and second-order systems, you can "piece together" a periodic solution by using simple techniques.

Example 1-13: Consider the RC network depicted by Figure 1-20 with R = 1 Ohm and C = 1 Farad. Suppose input x(t) is a T-periodic square wave that toggles between ±1. When x = 1, the capacitor is charging up, and the capacitor voltage is increasing exponentially with a time constant τ_0 = RC = 1 second. When x = -1, the capacitor is discharging, and the capacitor voltage is exponentially decreasing. Figure 1-21 depicts one period of the input and anticipated response. The peak output, α, must be computed.

From (1-147) with τ_0 = RC = 1 and y(0) = $-\alpha$, we can write

$$y(T/2) = e^{-T/2}\left[\int_0^{T/2} e^{\tau}d\tau - \alpha\right] = \alpha\,. \qquad (1\text{-}154)$$

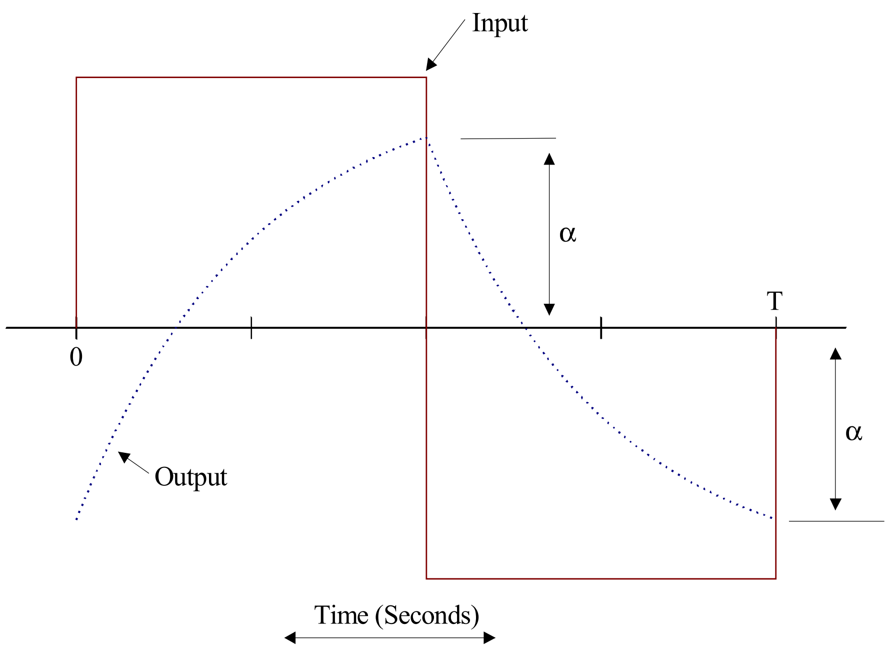

Figure 1-21: Square wave input shown as solid-line graph. RC circuit output shown as dashed line graph. Value of α is dependent on R, C and T, and it must be computed.

Integrate the exponential in (1-154) and obtain

$$\alpha = \frac{1-e^{-T/2}}{1+e^{-T/2}} \tag{1-155}$$

for α. Over the range $0 \le t \le T/2$, the output can be expressed as

$$y(t) = e^{-t}\left[\int_0^t e^{\tau}d\tau - \alpha\right] = 1-(1+\alpha)e^{-t}, \qquad 0 \le t \le T/2\,. \tag{1-156}$$

On the second-half of the period, the output can be expressed as

$$y(t) = e^{-(t-T/2)}\left[-\int_{T/2}^{t} e^{(\tau-T/2)}d\tau + \alpha\right] = -1+(1+\alpha)e^{-(t-T/2)}, \qquad T/2 \le t \le T\,. \tag{1-157}$$

In (1-156) and (1-157), use α given by (1-155). The T-periodic output is simply a periodic

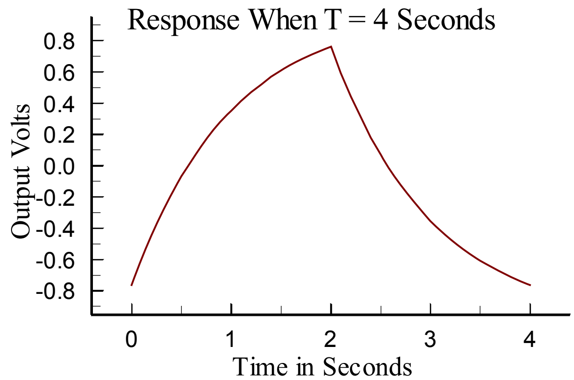

Figure 1-22: One period of the output for the case T = 4 seconds.

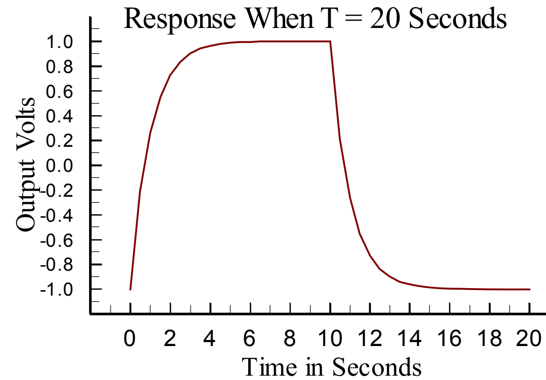

Figure 1-23: One period of the output for the case T = 20 seconds.

extension of the waveform described by (1-156) and (1-157). Figures 1-22 and 1-23 depict one period of the output for T = 4 and T = 20, respectively. The simple techniques that were used here for the RC circuit can be applied to a wide number of first- and second-order systems subjected to a wide variety of periodic inputs.

Ideal Low-Pass Filter

An *ideal low-pass filter* (LPF) has a transfer function given by

$$\begin{aligned} H_{lp}(\omega) &= Ae^{-j\omega t_0}, \quad -\omega_c < \omega < \omega_c \\ &= 0, \qquad\qquad \text{otherwise} \end{aligned}, \tag{1-158}$$

where $A > 0$, $t_0 > 0$ and bandwidth ω_c are known. Figure 1-24 depicts the magnitude and phase response of an ideal LPF. Within the pass band, the amplitude is constant and the phase is linear.

The impulse response of the ideal LPF is

$$h_{lp}(t) = \mathscr{F}^{-1}\left[H_{lp}(\omega)\right] = \frac{A\omega_c}{\pi}\frac{\sin\omega_c(t-t_0)}{(t-t_0)} = \frac{A\omega_c}{\pi}\text{Sa}\{\omega_c(t-t_0)\}, \tag{1-159}$$

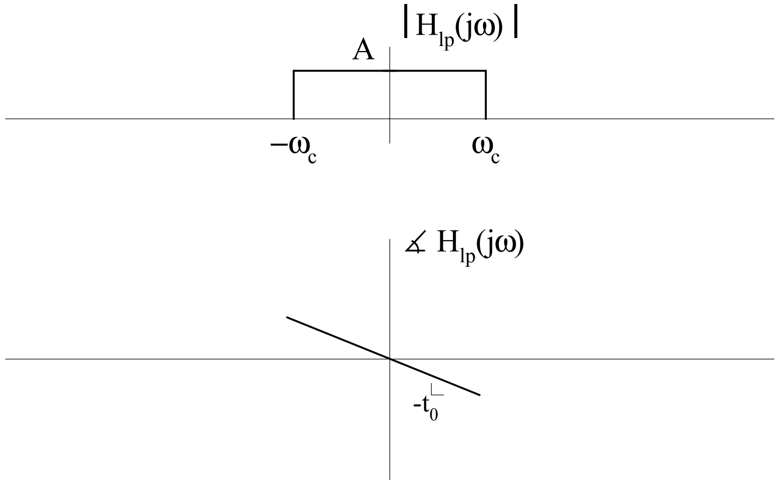

Figure 1-24: Magnitude and phase response of an ideal low-pass filter. A and t_0 are known quantities.

where Sa(x) = sin(x)/x. Figure 1-25 depicts the general form of (1-159). Note that the ideal LPF is non-causal, which implies that real-time, ideal low-pass filters cannot be implemented.

Ideal High-Pass Filter

An *ideal high-pass filter* (LPF) has a transfer function given by

$$\begin{aligned} H_{hp}(\omega) &= Ae^{-j\omega t_0}, \quad |\omega| > \omega_c \\ &= 0, \qquad\quad\;\; |\omega| < \omega_c \end{aligned}, \tag{1-160}$$

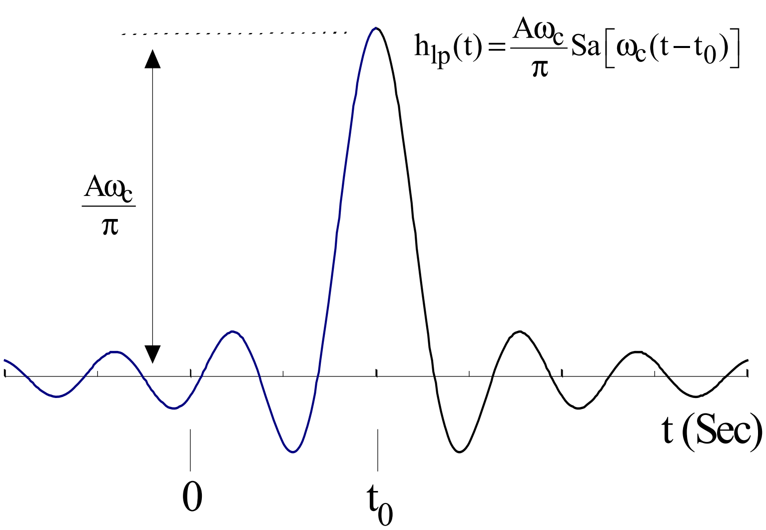

Figure 1-25: Impulse response of an ideal low-pass filter.

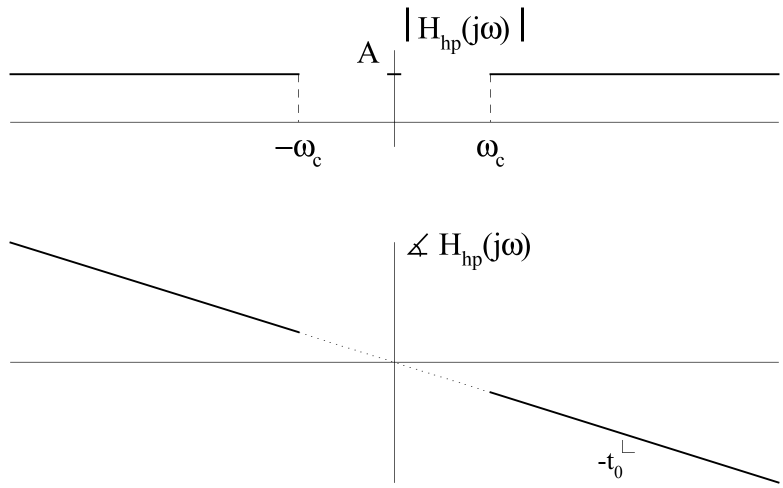

Figure 1-26: Transfer function of an ideal high-pass filter.

where A > 0, $t_0 > 0$ and ω_c are known. Figure 1-26 depicts the magnitude and phase response of an ideal HPF. Note that

$$H_{hp}(\omega) = Ae^{-j\omega_0 t} - H_{lp}(\omega)\,, \tag{1-161}$$

so that the impulse response of an ideal high-pass filter is given by

$$h_{hp}(t) = \mathscr{F}^{-1}\Big[H_{hp}(\omega)\Big] = A\delta(t - t_0) - \frac{A\omega_c}{\pi}\mathrm{Sa}\{\omega_c(t - t_0)\}\,, \tag{1-162}$$

as shown by Figure 1-27.

Ideal Band-Pass Filter

A band-pass filter passes signals contained in a band centered at some frequency ω_0. An *ideal band-pass filter* (BPF) has a transfer function given by

$$\begin{aligned} H_{bp}(\omega) &= Ae^{-j\omega t_0}, \quad \left|\omega - \omega_0\right| < \omega_c \quad \text{or} \quad \left|\omega + \omega_0\right| < \omega_c \\ &= 0, \quad\quad \text{otherwise} \end{aligned}\,, \tag{1-163}$$

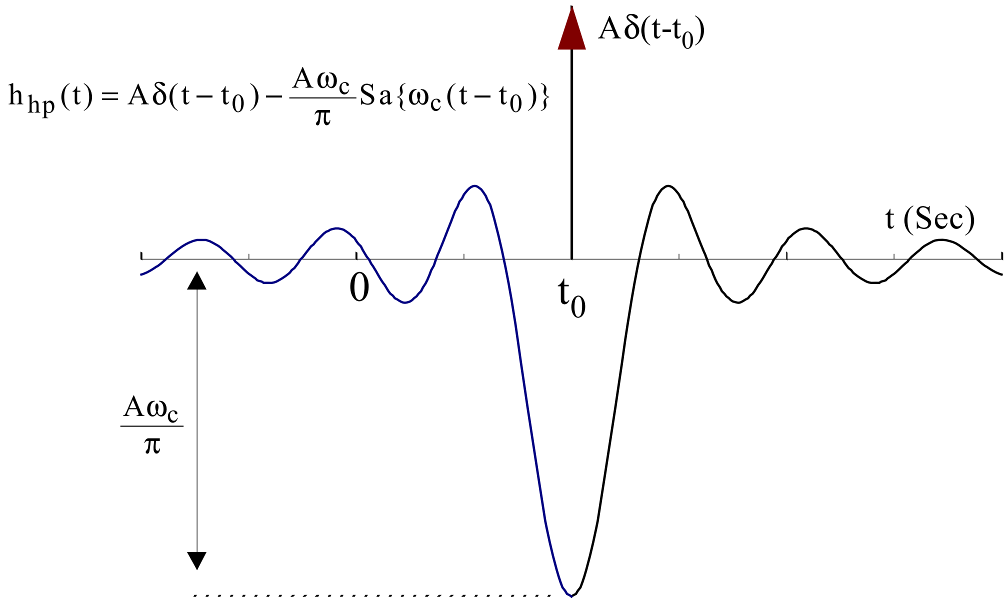

Figure 1-27: Impulse response of an ideal high-pass filter.

where $A > 0$, $t_0 > 0$, $\omega_0 > 0$ and $\omega_c > 0$ are known. Figure 1-28 depicts the magnitude and phase response of an ideal BPF. Note that

$$H_{bp}(\omega) = H_{lp}(\omega - \omega_0)e^{-j\omega_0 t_0} + H_{lp}(\omega + \omega_0)e^{+j\omega_0 t_0}\,, \tag{1-164}$$

so that the impulse response of an ideal high-pass filter is given by

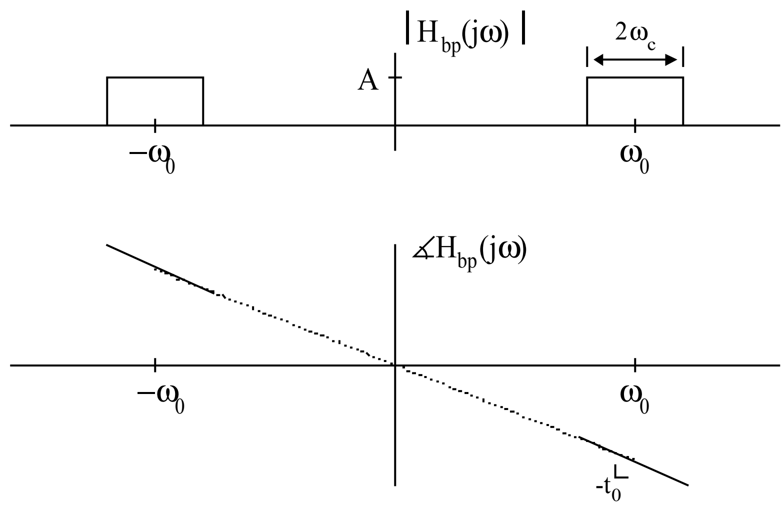

Figure 1-28: Magnitude and phase response of an ideal band-pass filter.

$$h_{bp}(t) = h_{lp}(t)e^{j\omega_0(t-t_0)} + h_{lp}(t)e^{-j\omega_0(t-t_0)} = 2h_{lp}(t)\left[\frac{e^{j\omega_0(t-t_0)} + e^{-j\omega_0(t-t_0)}}{2}\right], \tag{1-165}$$

$$= 2h_{lp}(t)\cos[\omega_0(t-t_0)]$$

see Figure 1-29.

Butterworth Low-Pass Filters

We describe the commonly-used n^{th}-order Butterworth filter. This is accomplished by stating the filter magnitude response, filter pole locations, and filter transfer function.

The squared magnitude function for an n^{th}-order Butterworth low-pass filter is

$$\left|H(j\omega)\right|^2 = H(j\omega)H^*(j\omega) = \frac{1}{1+(j\omega/j\omega_c)^{2n}}, \tag{1-166}$$

where constant ω_c is the 3dB cut-off frequency. Magnitude $|H(j\omega)|$ is depicted by Figure 1-30. It is easy to show that the first 2n-1 derivatives of $|H(j\omega)|^2$ at $\omega = 0$ are equal to zero. For this reason, we say that the Butterworth response is *maximally flat* at $\omega = 0$. Furthermore, the

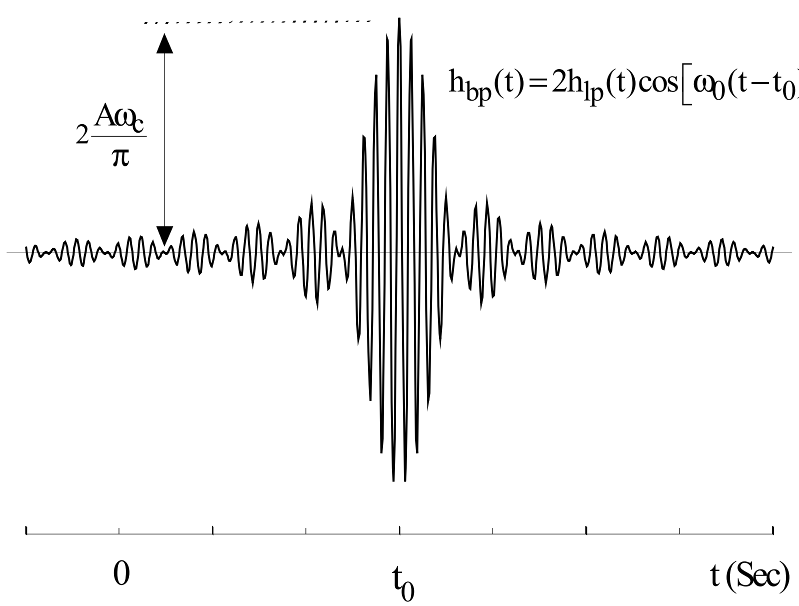

Figure 1-29: Impulse response of an ideal band-pass filter.

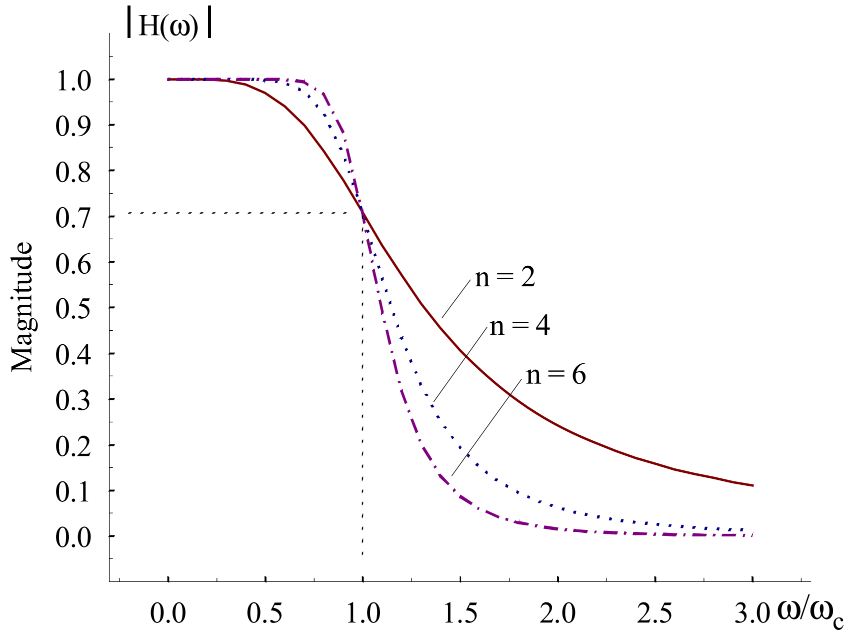

Figure 1-30: Magnitude response of an ideal n^{th}-order Butterworth filter.

derivative of the magnitude response is always negative for positive ω, the magnitude response is monotonically decreasing with increasing ω.

We require h(t) to be real-valued and causal. This requirement leads to

$$H^*(j\omega) = \left[\int_0^\infty h(t)e^{-j\omega t}dt\right]^* = \int_0^\infty h(t)e^{j\omega t}dt = H(-j\omega)\,, \tag{1-167}$$

so that

$$H(j\omega)H(-j\omega) = \frac{1}{1+(j\omega/\,j\omega_c)^{2n}}\,. \tag{1-168}$$

Note that there is no real value of ω for which H(ω) = ∞. That is, H(jω) has no poles on the jω-axis of the complex s-plane.

We require the filter to be causal and stable. Causality requires h(t) = 0, t < 0. Stability requires the causal impulse response to satisfy

$$\int_0^\infty |h(t)|\,dt < \infty\,. \tag{1-169}$$

Causality and stability requires that the time-invariant filter have all of its poles in the left-half of the complex s-plane (no jω-axis, or right-half-plane poles). The region of convergence for H(s) is of the form Re(s) > σ for some σ < 0, see Figure 1-31. Hence, H(s) can be obtained from H(jω), the Fourier transform of the impulse response, by replacing s with jω. In (1-168), replace jω with s to obtain

$$H(s)H(-s) = \frac{1}{1+(s/j\omega_c)^{2n}}\,. \tag{1-170}$$

As can be seen from inspection of (1-170), the poles of H(s)H(-s) are the roots of 1 + $(s/j\omega_c)^{2n} = 0$. That is, each pole must be one of the numbers

$$s_p = j\omega_c(-1)^{1/2n}\,. \tag{1-171}$$

There are 2n distinct values of s_p; they are found by multiplying the 2n roots of -1 by the complex constant $j\omega_c$.

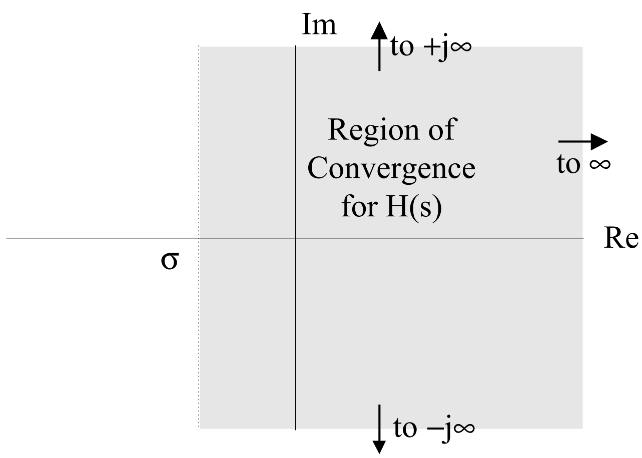

Figure 1-31: Region of convergence for transform H(s), the s-domain transfer function of a n^{th}-order Butterworth filter. Value σ < 0 depends on ω_c and n. All poles of H(s) must have a real part that is less than, or equal to σ.

The 2n roots of -1 are obtained easily. Complex variable z is a 2n root of -1 if

$$z^{2n} = -1. \tag{1-172}$$

Clearly, z must have unity magnitude and phase π/2n, modulo 2π/2n. Hence, the 2n roots of -1 form the set

$$\left[1\measuredangle\left\{\tfrac{\pi}{2n}+\tfrac{\pi}{n}k\right\},\ \ k = 0, 1, 2, \cdots, 2n\text{-}1\right] \tag{1-173}$$

Multiple these roots of -1 by $j\omega_c$ to obtain the poles of H(s)H(-s). This produces

$$p_k = \omega_c\measuredangle\left\{\tfrac{\pi}{2}+\tfrac{\pi}{2n}+\tfrac{\pi}{n}k\right\},\ \ k = 0, 1, 2, \cdots, 2n\text{-}1. \tag{1-174}$$

as the poles of H(s)H(-s). Notice that p_0, p_1, …, p_{n-1} are in the left-half of the complex plane, while p_n, …, p_{2n-1} are in the right-half plane. In the complex plane, these poles are on a circle (called the *Butterworth Circle*) of radius ω_c, and they are spaced π/n radians apart in angle. The poles given by (1-174) are

1) symmetric with respect to both axes,

2) never fall on the jω axis,

3) a pair falls on the real axis for n odd but not for n even,

4) lie on the *Butterworth circle* of radius ω_c where they are spaced π/n radians apart in angle, and

5) half of their number are in the right-half plane and half are in the left-half-plane.

Using (1-174), we can write

$$H(s)H(-s) = \frac{1}{1+(s/j\omega_c)^{2n}} = \frac{p_0 p_1 \cdots p_{2n-1}}{(s-p_0)(s-p_1)\cdots(s-p_{2n-1})}. \tag{1-175}$$

Since the poles of H(s) are in the left-half plane, we factor (1-175) to produce

$$H(s) = \frac{(-1)^n p_0 p_1 \cdots p_{n-1}}{(s-p_0)(s-p_1)\cdots(s-p_{n-1})}, \tag{1-176}$$

the transfer function of the nth-order Butterworth filter. So far, we have required a unity DC gain for the filter (*i.e.*, H(0) = 1). However, any DC gain can be obtained by simply multiplying (1-176) by the correct constant.

Example 1-14: Determine the transfer function for a unity-DC-gain, third-order Butterworth filter with a cut-off frequency of ω_c = 1 radian/second. The Butterworth circle and 6 poles of H(s)H(-s) are depicted by Figure 1-32. The poles of H(s) are given by (1-174); these numbers are

$$\begin{aligned} &p_0 = 1\measuredangle\{\pi/2+\pi/6\} = 1\measuredangle\tfrac{2\pi}{3}, \qquad p_1 = 1\measuredangle\{\pi/2+\pi/6+\pi/3\} = 1\measuredangle\pi \\ &p_2 = 1\measuredangle\{\pi/2+\pi/6+2\pi/3\} = 1\measuredangle-\tfrac{2\pi}{3} \end{aligned} \quad . \tag{1-177}$$

Finally, the s-domain transfer function is given by

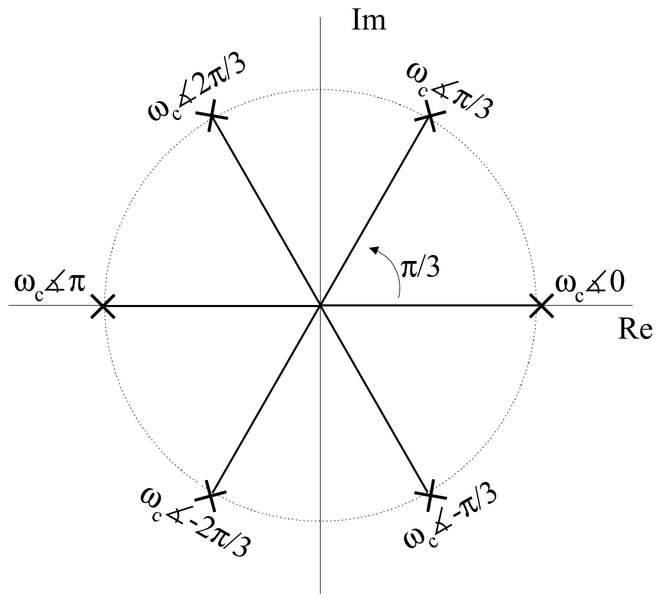

Figure 1-32: Butterworth circle of radius ω_c = 1 for a third-order filter.

$$H(s) = \frac{1}{(s-1\measuredangle\frac{2\pi}{3})(s-1\measuredangle\pi)(s-1\measuredangle-\frac{2\pi}{3})} = \frac{1}{s^3+2s^2+2s+1}. \tag{1-178}$$

The Matlab Signal Processing Toolbox has several powerful functions that are useful for designing Butterworth (and other types of) filters. For example, the code

```
N = 3;
W = 1;
[num,den] = butter(N,W,'s')
```

will design the 3rd-order Butterworth filter that is discussed in this example. N is the filter order. W is the 3dB cut-off frequency, `num` is a 1×3 vector of numerator coefficients, and `dom` is a 1×3 vector of denominator coefficients (the coefficient vectors are ordered highest to lowest power of s). To try out "butter", one can type `[num,den]=butter(3,1,'s') at` the Matlab command prompt to obtain

```
>> [num,den]=butter(3,1,'s')
num =
         0         0         0    1.0000
den =
    1.0000    2.0000    2.0000    1.0000
>>
```

Notice that Matlab returns numerator and denominator polynomial coefficients that agree with the right-hand side of (1-178).

Hilbert Transforms

Consider the filter H(jω), described by Figure 1-33, that has a unity magnitude response for all frequencies. Also, the phase response is -π/2 for positive frequencies and π/2 for negative frequencies. The transfer function of this filter is

$$H(j\omega) = -j\,\mathrm{sgn}(\omega). \tag{1-179}$$

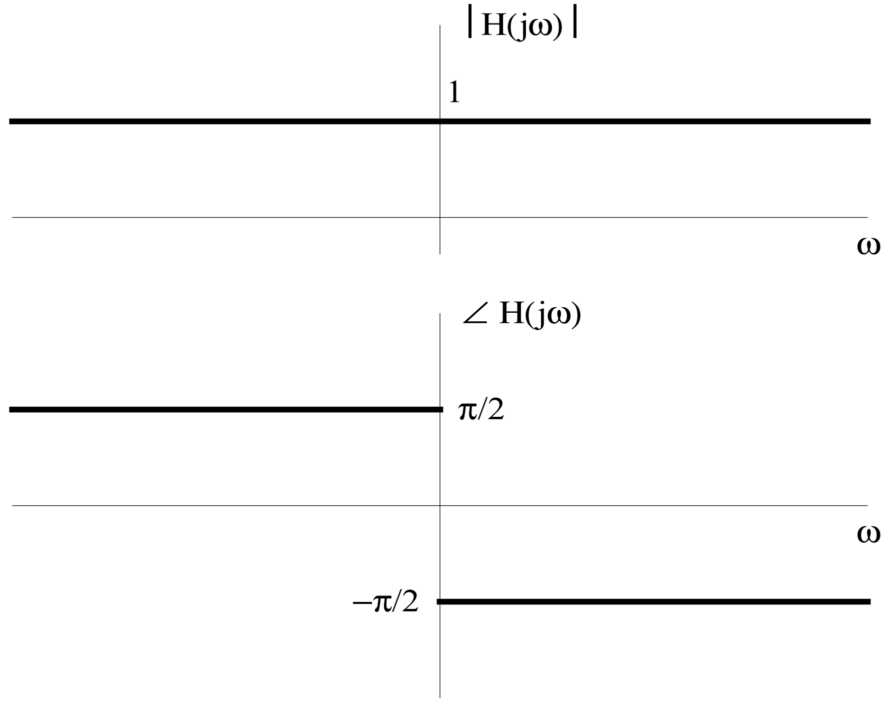

Figure 1-33: Magnitude and phase of Hilbert transform operator.

An engineer might think of a Hilbert transform as a "wide-band, 90 degree phase shift network".

The impulse response of the filter is

$$h(t) = \mathcal{F}^{-1}[H] = -j\mathcal{F}^{-1}[\text{sgn}(\omega)] = -j\left(\frac{j}{\pi t}\right) = \frac{1}{\pi t}, \tag{1-180}$$

a result depicted by Figure 1-34. Note that the filter is non-causal. When driven by an arbitrary signal x(t), the filter produces the output

$$\hat{x}(t) = x * h = \int_{-\infty}^{\infty} \frac{x(u)}{\pi(t-u)}\, du \tag{1-181}$$

The function $\hat{x}(t)$ is the *Hilbert Transform* of x(t). Note that

$$\mathcal{F}[\hat{x}] = H(\omega)X(\omega) = -j\,\text{sgn}(\omega)X(\omega), \tag{1-182}$$

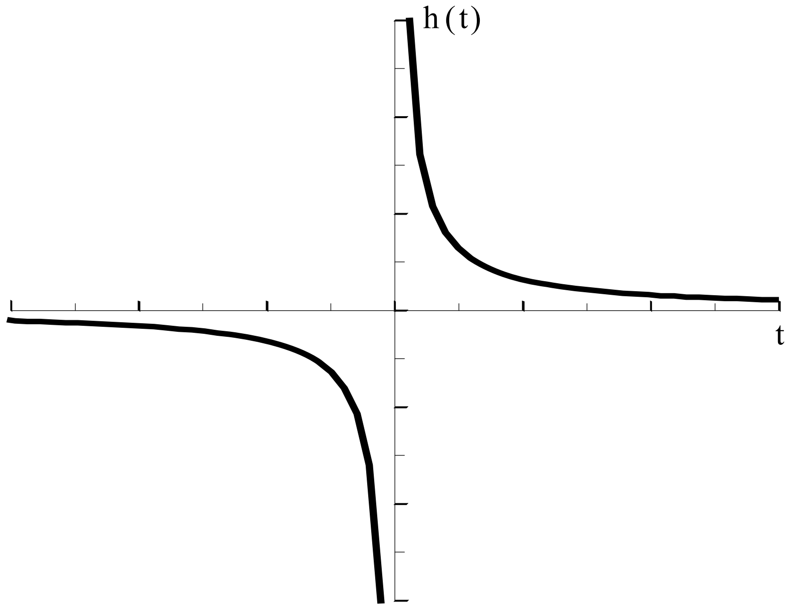

Figure 1-34: Impulse response h(t) of Hilbert transform operator.

so that

$$\hat{x}(t) = \mathcal{F}^{-1}\left[-j\,\mathrm{sgn}(\omega)X(\omega)\right]. \tag{1-183}$$

In some cases, this formula allows use of a Fourier transform table to compute the Hilbert transform.

Example 1-15: Consider x(t) = cos(ω_0t) with transform X(jω) = $\pi[\delta(\omega - \omega_0) + \delta(\omega + \omega_0)]$. We have

$$\begin{aligned} -j\,\mathrm{sgn}(\omega)X(\omega) &= j\pi\left[\delta(\omega+\omega_0) - \delta(\omega-\omega_0)\right],\ \omega_0 > 0 \\ &= j\pi\left[\delta(\omega-\omega_0) - \delta(\omega+\omega_0)\right],\ \omega_0 < 0 \end{aligned}$$

so that -jsgn(ω)X(jω) = $j\pi[\delta(\omega + \omega_0) - \delta(\omega - \omega_0)]\mathrm{sgn}(\omega_0)$. Hence, we can write

$$\hat{x}(t) = \widehat{\cos\omega_0 t} = \mathcal{F}^{-1}\left[-j\,\mathrm{sgn}(\omega)X(j\omega)\right] = \mathrm{sgn}(\omega_0)\sin\omega_0 t \tag{1-184}$$

Example 1-16: In a similar manner, we can write

$$\widehat{\sin\omega_0 t} = -\operatorname{sgn}(\omega_0)\cos\omega_0 t \tag{1-185}$$

Example 1-17: Combine (1-184) and (1-185) to obtain

$$\widehat{\exp\{j\omega_0 t\}} = \widehat{\cos\omega_0 t + j\sin\omega_0 t} = \operatorname{sgn}(\omega_0)[\sin\omega_0 t - j\cos\omega_0 t] = -j\operatorname{sgn}(\omega_0)\exp\{j\omega_0 t\} \tag{1-186}$$

Properties of Hilbert Transforms

1. The energy (or power) in x(t) and $\hat{x}(t)$ are equal. This claim follows from

$$\left|\mathcal{F}[\hat{x}]\right|^2 = \left|-j\operatorname{sgn}(\omega)X(\omega)\right|^2 = \left|X(\omega)\right|^2 = \left|\mathcal{F}[x]\right|^2. \tag{1-187}$$

Since the energy (or power) density spectrum at the input and output of the filter are the same, the two energies (or powers) are equal.

2. $\hat{\hat{x}}(t) = -x(t)$. This claim follows from

$$\begin{aligned}\hat{\hat{x}}(t) &= \mathcal{F}^{-1}\left[-j\operatorname{sgn}(\omega)\mathcal{F}[\hat{x}(t)]\right]\\ &= \mathcal{F}^{-1}\Big[-j\operatorname{sgn}(\omega)\big[-j\operatorname{sgn}(\omega)X(j\omega)\big]\Big]\\ &= \mathcal{F}^{-1}\left[-X(j\omega)\right]\\ &= -x(t)\end{aligned}. \tag{1-188}$$

3. x(t) and $\hat{x}(t)$ are orthogonal. For energy signals, we have

$$\lim_{T\to\infty}\int_{-T}^{T} x(t)\hat{x}(t)dt = 0. \tag{1-189}$$

For power signals, we have

$$\langle x(t)\hat{x}(t)\rangle \equiv \underset{T\to\infty}{\text{limit}} \frac{1}{2T}\int_{-T}^{T} x(t)\hat{x}(t)dt = 0\,. \tag{1-190}$$

This claim follows from (proof given for energy signals; proof for power signals is similar)

$$\begin{aligned}\int_{-\infty}^{\infty} x(t)\hat{x}(t)dt &= \int_{-\infty}^{\infty} x(t)\left[\frac{1}{2\pi}\int_{-\infty}^{\infty} -j\,\text{sgn}(\omega)X(j\omega)e^{j\omega t}d\omega\right]dt \\ &= \frac{1}{2\pi}\int_{-\infty}^{\infty} -j\,\text{sgn}(\omega)X(j\omega)\left[\int_{-\infty}^{\infty} x(t)e^{j\omega t}dt\right]d\omega \\ &= \frac{-j}{2\pi}\int_{-\infty}^{\infty} \text{sgn}(\omega)\left|X(j\omega)\right|^2 d\omega \\ &= 0\end{aligned} \tag{1-191}$$

since integrand sgn(ω)$|X(j\omega)|^2$ is an odd function which is integrated over symmetric limits.

4. If c(t) and m(t) are signals with non-overlapping spectra, where m(t) is low pass and c(t) is high pass, then

$$\widehat{m(t)c(t)} = m(t)\hat{c}(t) \tag{1-192}$$

To develop this important result, denote **M**(jω) = $\mathcal{F}$[m(t)] and **C**(jω) = $\mathcal{F}$[c(t)] as the Fourier transform of m and c, respectively. The fact that the signals have no over-lapping spectrum implies that there exists a W for which

$$\begin{aligned}\mathbf{M}(\omega) &= \mathcal{F}\left[m(t)\right] = 0,\ \ |\omega| > W \\ \mathbf{C}(\omega) &= \mathcal{F}\left[c(t)\right] = 0,\ \ |\omega| < W\end{aligned} \tag{1-193}$$

since m(t) is low pass and c(t) is high pass. Use (1-193) and note that

$$\begin{aligned}\widehat{m(t)c(t)} &= \frac{1}{(2\pi)^2}\int_{-\infty}^{\infty}\int_{-\infty}^{\infty}\mathbf{M}(j\omega_1)\mathbf{C}(j\omega_2)\widehat{\exp[j(\omega_1+\omega_2)t]}\,d\omega_1 d\omega_2 \\ &= \frac{1}{(2\pi)^2}\int_{-\infty}^{\infty}\int_{-\infty}^{\infty}\mathbf{M}(j\omega_1)\mathbf{C}(j\omega_2)[-j\,\mathrm{sgn}(\omega_1+\omega_2)]\exp[j(\omega_1+\omega_2)t]\,d\omega_1 d\omega_2\end{aligned} \quad . \qquad (1\text{-}194)$$

Once the quantity $\mathrm{sgn}(\omega_1 + \omega_2)$ in the integrand of (1-194) is simplified, we will obtain the desired result. To simplify (1-194), note that non-overlapping spectra and (1-193) imply

$$\begin{aligned}&\mathbf{M}(\omega_1) = 0, \ |\omega_1| > W \\ &\mathbf{C}(\omega_2) = 0, \ |\omega_2| < W\end{aligned} \quad . \qquad (1\text{-}195)$$

Hence, the integrand of (1-194) is zero for all (ω_1, ω_2) in the cross-hatched region on Fig 1-35. More importantly, on the shaded region of the (ω_1, ω_2) plane, the integrand is non-zero, and we can write

$$\mathrm{sgn}(\omega_1 + \omega_2) = \mathrm{sgn}(\omega_2) \qquad (1\text{-}196)$$

for all (ω_1, ω_2) in the shaded (but not the cross-hatched!) region illustrated on Figure 1-35. Finally, use of simplification (1-195) in Equation (1-194) yields the desired result

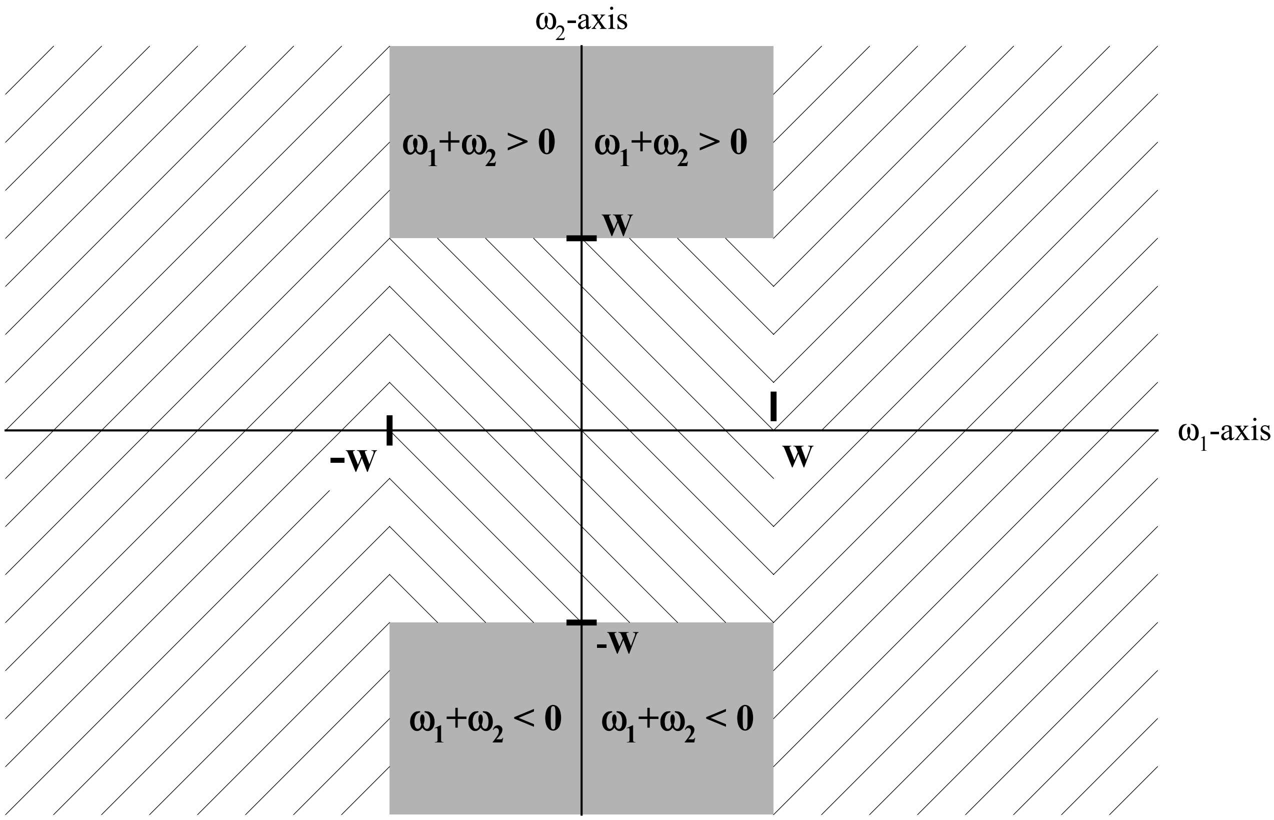

Figure 1-35: Integrand of **(1-194)** is zero in the cross-hatched region. In the upper-half plane shaded region, we have $U(\omega_1 + \omega_2) = 1$. In the lower-half plane shaded region, we have $U(\omega_1 + \omega_2) = -1$.

$$\begin{aligned} m(t)c(t) &= \left[\frac{1}{2\pi}\int_{-\infty}^{\infty} \mathbf{M}(\omega_1)\exp[j\omega_1 t]d\omega_1\right]\left[\frac{1}{2\pi}\int_{-\infty}^{\infty} \mathbf{C}(\omega_2)[-j\,\mathrm{sgn}(\omega_2)]\exp[j\omega_2 t]\,d\omega_2\right] \\ &= m(t)\hat{c}(t) \end{aligned}$$

which is (1-192).

5. Since the impulse response h(t) does not vanish for t < 0, *the Hilbert transform is a non-causal linear operator*.

6. If x(t) is an even (alternatively, odd) function then $\hat{x}(t)$ is an odd (alternatively, even) function.

Proof: This claim follows easily from Fourier transform theory. If x(t) is an even function of t, then we have

$$X(j\omega) = \int_{-\infty}^{\infty} x(t)e^{-j\omega t}dt = \int_{-\infty}^{\infty} x(t)\cos\omega t\,dt - j\int_{-\infty}^{\infty} x(t)\sin\omega t\,dt = \int_{-\infty}^{\infty} x(t)\cos\omega t\,dt\,, \tag{1-197}$$

an even function of ω. Hence, -jsgn(ω)X(jω) is an odd function of ω. As a result, we have

$$\begin{aligned}\hat{x}(t) &= \mathcal{F}^{-1}\left[-j\,\mathrm{sgn}(\omega)X(j\omega)\right] = \frac{1}{2\pi}\int_{-\infty}^{\infty}\{-j\,\mathrm{sgn}(\omega)X(j\omega)\}e^{j\omega t}d\omega \\ &= \frac{1}{2\pi}\int_{-\infty}^{\infty}\mathrm{sgn}(\omega)X(j\omega)\sin\omega t\,d\omega\end{aligned} \tag{1-198}$$

as an odd function of t.

Analytic Signal

Let x(t) be a real-valued signal. The *analytic signal* (also called the *pre-envelope*) for x(t) is defined as

$$x_p(t) \equiv x(t) + j\hat{x}(t)\,. \tag{1-199}$$

The analytic signal for any given signal is denoted by placing a subscript p on the symbol that represents the signal (*i.e.,* corresponding to signal z is an analytic signal denoted by z_p). The analytic signal is used in the analysis of communication systems. Note that x_p can be written as

$$x_p(t) = x(t) * 2\left[\tfrac{1}{2}\delta(t) + j\tfrac{1}{2\pi t}\right] \tag{1-200}$$

Hence, the Fourier transform of x_p is

$$X_p(j\omega) \equiv \mathcal{F}\left[x_p\right] = \mathcal{F}\left[x(t)\right]\cdot 2\mathcal{F}\left[\tfrac{1}{2}\delta(t) + j\tfrac{1}{2\pi t}\right] = 2X(j\omega)U(\omega)\,, \tag{1-201}$$

where U(ω) is a unit step in the frequency domain. On x_p and X_p, the subscript p denotes the "positive part".

Given any real-valued signal x(t), we define

$$x_n(t) \equiv x(t) - j\hat{x}(t). \tag{1-202}$$

The Fourier transform of x_n is

$$X_n(j\omega) \equiv \mathcal{F}\left[x_n\right] = \mathcal{F}\left[x(t)\right] \cdot 2\mathcal{F}\left[\tfrac{1}{2}\delta(t) - j\tfrac{1}{2\pi t}\right] = 2X(j\omega)U(-\omega). \tag{1-203}$$

On x_n and X_n, the subscript n denotes the “negative part”.

Narrow-Band Signals and Systems

Narrow-band signals and systems play an important role in communication systems. Practically all radio-frequency-based communication systems (*i.e.*, radio and TV broadcasting, civil, military and amateur radio communication systems, etc.) utilize narrow-band signals and systems. This section contains some general modeling techniques for narrow-band signals and systems.

Modeling Band-Pass Signals and Systems

A real-valued band-pass signal $x_{bp}(t)$ can be represented as

$$x_{bp}(t) = \Gamma(t)\cos(\omega_c t + \phi(t)), \tag{1-204}$$

where Γ and ϕ are known as the *envelope* and *phase*, respectively, of the signal. Also, constant ω_c is known as the *carrier frequency* of the signal. This equation can be written as

$$x_{bp}(t) = x_c(t)\cos\omega_c t - x_s(t)\sin\omega_c t, \tag{1-205}$$

where

$$x_c(t) = \Gamma(t)\cos\phi(t)$$
$$x_s(t) = \Gamma(t)\sin\phi(t)\,. \tag{1-206}$$

The quantities x_c and x_s are the *quadrature components* of x_{bp}.

Signal x_{bp} is said to be *narrow-band* if it has a bandwidth which is small compared to ω_c. The quadrature components x_c and x_s vary slowly relative to $\cos\omega_c t$. Over any period of $\cos\omega_c t$, the quadrature components are nearly constant; many periods of $\cos\omega_c t$ must occur before there is appreciable change in x_c and/or x_s. Equivalently, x_c and x_s are low-pass processes with bandwidths that are small compared to ω_c.

Linear, time-invariant band-pass systems can be treated in much the same manner as narrow-band signals. Such a system has an impulse response that can be written as

$$h_{bp}(t) = h_c(t)\cos\omega_c t - h_s(t)\sin\omega_c t\,, \tag{1-207}$$

where h_c and h_s are real-valued, low-pass functions. Equations (1-206) and (1-207) have similar forms; hence, many of the formal manipulations outlined below can be applied to both band-pass signals and systems.

A simple example of a narrow-band system, that is used as a filter in many applications, is depicted by Fig. 1-36. The transfer function of this simple network is given by

$$H_{bp}(s) = \frac{2\alpha_0 s}{(s+\alpha_0)^2 + \omega_c^2} = 2\alpha_0\left[\frac{s+\alpha_0}{(s+\alpha_0)^2 + \omega_c^2}\right] - \frac{2\alpha_0^2}{\omega_c}\left[\frac{\omega_c}{(s+\alpha_0)^2 + \omega_c^2}\right], \tag{1-208}$$

where $\alpha_0 \equiv R/2L$, $\omega_c \equiv (\omega_n^2 - \alpha_0^2)^{1/2}$, and $\omega_n \equiv (1/LC)^{1/2}$. In most applications, the component values are chosen so that the narrow-band condition $\omega_n^2 >> \alpha_0^2$ applies and $\omega_c \approx \omega_n$. This filter has the narrow-band impulse response

$$h_{bp}(t) = \mathscr{L}^{-1}\left[H_{bp}(s)\right] = 2\alpha_0 e^{-\alpha_0 t}\left[\cos\omega_c t - \frac{\alpha_0}{\omega_c}\sin\omega_c t\right]U(t)\,. \tag{1-209}$$

Here, the quadrature components are

$$\begin{aligned} h_c(t) &\equiv 2\alpha_0 \exp(-\alpha_0 t)\,U(t) \\ h_s(t) &\equiv \frac{2\alpha_0^2}{\omega_c}\exp(-\alpha_0 t)\,U(t), \end{aligned} \tag{1-210}$$

where U(t) denotes the unit step function.

Low-Pass Equivalent Signals and Systems

Consider the band-pass signal (1-205). This band-pass function has a corresponding *low-pass equivalent* (also known as *complex envelope*) function defined by

$$x_{lp}(t) \equiv x_c(t) + j\,x_s(t)\,. \tag{1-211}$$

The band-pass function x_{bp} can be written in terms of x_{lp} as

$$x_{bp}(t) = \mathrm{Re}[x_{lp}(t)\exp(j\omega_c t)]\,, \tag{1-212}$$

where Re denotes that only the real part of the bracketed expression should be retained. As

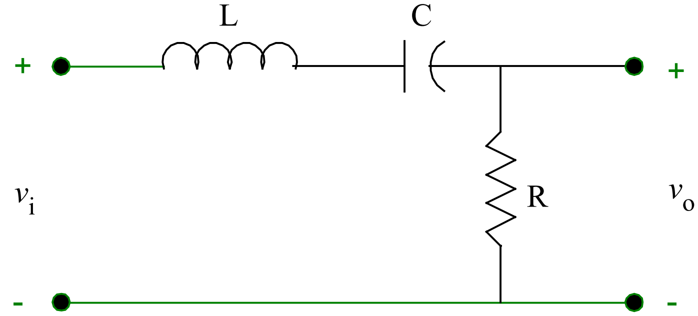

Figure 1-36: A simple band-pass filter.

shown below, use of low-pass equivalents simplifies analysis involving band-pass signals and systems.

A simple relationship can be developed between the Fourier transforms of x_{lp} and x_{bp}. Equation (1-212) can be written as

$$x_{bp}(t) = \frac{1}{2}[x_{lp}(t)\exp(j\omega_c t) + x_{lp}^*(t)\exp(-j\omega_c t)], \tag{1-213}$$

and the Fourier transform of this signal is (since $x_{lp}^*(t) \leftrightarrow X_{lp}^*(-j\omega)$)

$$X_{bp}(j\omega) = \frac{1}{2}[X_{lp}(j\omega - j\omega_c) + X_{lp}^*(-j\omega - j\omega_c)], \tag{1-214}$$

where X_{lp} denotes the Fourier transform of x_{lp}. Now, all of the frequency components of low-pass $X_{lp}(j\omega)$ lie within a band whose upper frequency is small compared to ω_c. Hence, Equation (1-214) leads to the results

$$X_{bp}(j\omega)U(\omega) = \frac{1}{2}X_{lp}(j\omega - j\omega_c), \tag{1-215}$$

where $U(\omega)$ is the unit step function. Equation (1-215) shows how to use X_{lp} to obtain the positive-frequency side of X_{bp} (use known symmetries to obtain $X_{bp}(\omega)$, $-\infty < \omega < \infty$). Alternatively, Equation (1-215) can be used to write

$$X_{lp}(j\omega) = 2X_{bp}(j\upsilon)U(\upsilon)\Big|_{\upsilon = \omega + \omega_c}, \tag{1-216}$$

a formula for X_{lp} in terms of X_{bp}. Equation (1-216) serves as the basis of Fig. 1-37 which illustrates the relationship between the magnitude and phase of X_{lp} and X_{bp}.

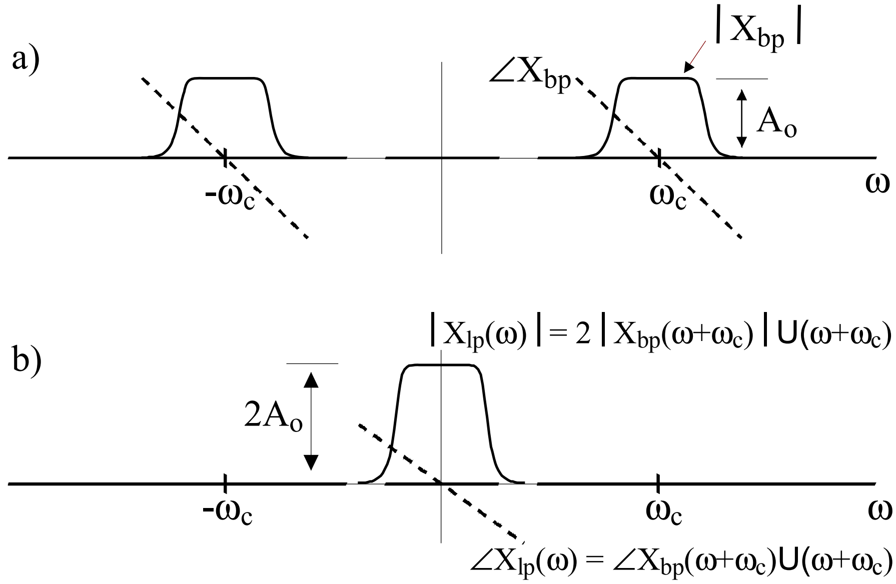

Figure 1-37: Magnitude and phase of a) band-pass signal and b) its low-pass equivalent.

Equation (1-211) defines the low-pass function x_{lp} in terms of the quadrature components of bandpass x_{bp}. However, x_{lp} can be expressed directly in terms of this band-pass process. Take the inverse Fourier transform of (1-216) and obtain

$$\begin{aligned} x_{lp}(t) &= \frac{1}{2\pi}\Big[x_{bp}(t) * 2\mathcal{F}^{-1}[U(\omega)]\Big]\exp(-j\omega_c t) = \Big[x_{bp}(t) * [\,\delta(t) + j\frac{1}{\pi t}\,]\Big]\exp(-j\omega_c t) \\ &= \Big[x_{bp}(t) + j\hat{x}_{bp}(t)\Big]\exp(-j\omega_c t), \end{aligned} \tag{1-217}$$

where $\hat{x}_{bp}$ denotes the *Hilbert transform* of band-pass process x_{bp}. In (1-217), the quantity x_{bp} + $j\hat{x}_{bp}$ is the *analytic signal* corresponding to x_{bp}; Equation (1-217) shows that x_{lp} is the analytic signal translated down to base-band. Conversely, the analytic signal corresponding to x_{bp} is just the low-pass equivalent x_{lp} translated up to the carrier frequency (multiply both sides of (1-217) by $\exp(j\omega_c t)$ to see this).

Symmetrical Band-Pass Filter

The magnitude (alternatively, phase) response of a *symmetrical band-pass filter* has ω_c as an axis of even (alternatively, odd) symmetry. That is, the filter transfer function satisfies

$$\begin{aligned} \left| H_{bp}(j\omega_c + j\omega) \right| &= \left| H_{bp}(j\omega_c - j\omega) \right| \\ \angle H_{bp}(j\omega_c + j\omega) &= -\angle H_{bp}(j\omega_c - j\omega) \end{aligned} \tag{1-218}$$

for $|\omega| < \omega_c$. Figure 1-37 illustrates magnitude and phase functions that satisfy (1-218). Not all band-pass filter transfer functions satisfy (1-218). However, as discussed next, band-pass signal and system analysis can be simplified when condition (1-218) holds (or can be assumed).

A symmetrical band-pass filter has a relatively simple impulse response. As can be seen from (1-216), its low-pass equivalent $H_{lp}(j\omega)$ has an even magnitude and an odd phase response. This implies that low-pass equivalent $h_{lp}(t) \equiv \mathcal{F}^{-1}[H_{lp}(j\omega)]$ is real-valued, and the band-pass filter impulse response has the form

$$h_{bp}(t) = h_c(t)\cos\omega_c t\,. \tag{1-219}$$

The converse is also true; if $h_{bp}(t)$ has the form given by (1-219) then the filter is symmetrical.

Example 1-18: Consider again the band-pass filter depicted by Figure 1-36. Under the conditions $\omega_c >> \alpha_0$, Equation (1-210) implies that $|h_s(t)| << |h_c(t)|$ for all time t, so that $h_{bp}(t)$ can be approximated as

$$h_{bp}(t) \approx 2\alpha_0 e^{-\alpha_0 t}\{\cos\omega_c t\}\ U(t)\,. \tag{1-220}$$

The filter described by (1-220) is symmetrical. Often, the condition that $\omega_c >> \alpha_0$ is called the *high Q*, or *narrow-band* condition.

Band-Pass Input/Output

Apply signal x_{bp}, described by (1-205), to the filter h_{bp}, described by (1-207), to obtain the band-pass output y_{bp}. Clearly, y_{bp} can be obtained by convolving x_{bp} and h_{bp}. However, this is a messy and laborious operation involving the products of several trigonometric functions. As outlined below, a much easier approach to this problem utilizes low-pass equivalent functions.

Let y_{lp} denote the low-pass equivalent of the filter band-pass output. As shown in this section, y_{lp} can be computed as

$$y_{lp} = \frac{1}{2} x_{lp} * h_{lp}, \tag{1-221}$$

a computation that uses only low-pass functions. Of course, once Equation (1-221) is used to obtain y_{lp}, the filter band-pass output can be computed as

$$y_{bp}(t) = \mathrm{Re}[\, y_{lp}(t) \exp(\, j\omega_c \, t)] \,. \tag{1-222}$$

This simplified approach to band-pass input/output computations is summarized by Fig. 1-38.

The derivation of (1-221) is straightforward. First, note that

$$\begin{aligned} y_{bp} &= x_{bp} * h_{bp} = \mathrm{Re}\left[x_{lp} e^{j\omega_c t} \right] * \mathrm{Re}\left[h_{lp} e^{j\omega_c t} \right] \\ &= \left[\frac{x_{lp} e^{j\omega_c t} + x_{lp}^{*} e^{-j\omega_c t}}{2} \right] * \left[\frac{h_{lp} e^{j\omega_c t} + h_{lp}^{*} e^{-j\omega_c t}}{2} \right], \end{aligned} \tag{1-223}$$

a computation requiring the convolution of four band-pass functions. Two of the convolutions involve functions of the same frequency (either $+\omega_c$ or $-\omega_c$). The convolution of the two $+\omega_c$ functions is

$$\left(x_{lp}e^{+j\omega_c t}\right)*\left(h_{lp}e^{+j\omega_c t}\right)=\int_{-\infty}^{\infty}x_{lp}(\tau)e^{+j\omega_c\tau}h_{lp}(t-\tau)e^{+j\omega_c(t-\tau)}d\tau=\left(x_{lp}*h_{lp}\right)e^{+j\omega_c t}. \tag{1-224}$$

Note that this convolution of band-pass signals is represented as a convolution of low-pass signals *multiplied* by a complex exponential. Likewise, the convolution of the two $-\omega_c$ functions is

$$\left(x_{lp}^{*}e^{-j\omega_c t}\right)*\left(h_{lp}^{*}e^{-j\omega_c t}\right)=\left(x_{lp}^{*}*h_{lp}^{*}\right)e^{-j\omega_c t}. \tag{1-225}$$

The two convolutions of opposite-sign frequency functions (one at $+\omega_c$ and the other at $-\omega_c$) is zero. To see this, note that

$$\begin{aligned}\left(x_{lp}e^{j\omega_c t}\right)*\left(h_{lp}^{*}e^{-j\omega_c t}\right)&=\int_{-\infty}^{\infty}x_{lp}(\tau)e^{j\omega_c\tau}h_{lp}^{*}(t-\tau)e^{-j\omega_c(t-\tau)}d\tau\\&=\left[\int_{-\infty}^{\infty}x_{lp}(\tau)e^{j2\omega_c\tau}h_{lp}^{*}(t-\tau)d\tau\right]e^{-j\omega_c t}\\&=\left[\left(x_{lp}(t)e^{j2\omega_c t}\right)*h_{lp}^{*}(t)\right]e^{-j\omega_c t}\\&\approx 0.\end{aligned} \tag{1-226}$$

Now, on the right hand side of (1-226), the convolution in the bracket is that of a narrow-band signal at $2\omega_c$ with a low-pass filter. The result can be taken as zero since $2\omega_c$ is very large compared to the cut off frequency of the low-pass h_{lp}. In a similar manner, we find that

$$\left(x_{lp}^{*}e^{-j\omega_c t}\right)*\left(h_{lp}e^{j\omega_c t}\right)\approx 0. \tag{1-227}$$

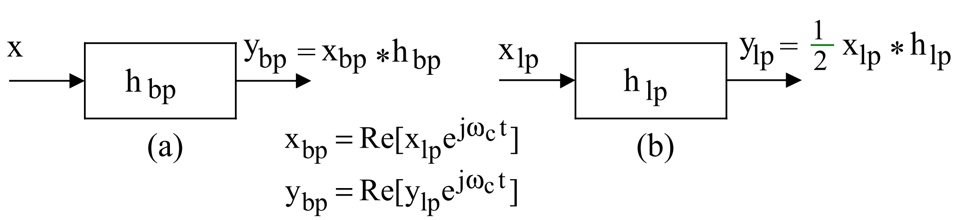

Figure 1-38: Input/output relationships for a) band-pass functions, and b) low-pass functions.

Equation (1-223) can be simplified by using these approximations. Substitute (1-224) through (1-227) into (1-223) to obtain

$$\begin{aligned} y_{bp} &= x_{bp} * h_{bp} = \frac{1}{4}(x_{lp} * h_{lp})e^{j\omega_c t} + \frac{1}{4}(x_{lp}^* * h_{lp}^*)e^{-j\omega_c t} \\ &= 2\,\mathrm{Re}\left[\frac{1}{4}(x_{lp} * h_{lp})e^{j\omega_c t}\right] = \mathrm{Re}\left[\frac{1}{2}(x_{lp} * h_{lp})e^{j\omega_c t}\right]. \end{aligned} \tag{1-228}$$

Comparing $y_{bp} = \mathrm{Re}\left[y_{lp}e^{j\omega_c t}\right]$ with (1-228), we arrive at the desired conclusion

$$y_{lp} = \frac{1}{2}x_{lp} * h_{lp}, \tag{1-229}$$

a result that is summarized by Fig. 1-38.

Example 1-19: Consider the band-pass filter depicted by Fig. 1-36. Assume that this filter has an input given by

$$x_{bp}(t) = x_c(t)\cos\omega_c t, \tag{1-230}$$

where

$$x_c(t) = \begin{cases} 1, & 0 \le t \le t_0 \\ 0, & \text{elsewhere}. \end{cases} \tag{1-231}$$

In many applications, this filter is designed so that $1/LC >> (R/2L)^2$. Under this condition, the frequency ω_c is approximately equal to $1/\sqrt{LC}$, and the filter has a high "Q". This high circuit "Q" condition is assumed to hold here. As can be seen from (1-210), the high circuit "Q" assumption implies that $h_c(t) >> h_s(t)$ for all time so that

$$h_{lp}(t) \approx 2\alpha_0 \exp(-\alpha_0 t)\, U(t)\,, \tag{1-232}$$

and a symmetrical filter can be assumed. Apply (1-229) to the last two equations and obtain

$$y_{lp}(t) = \begin{cases} 1 - \exp(-\alpha_0 t) & , \quad 0 \le t \le t_0 \\ [\exp(\alpha_0 t_0) - 1]\exp(-\alpha_0 t)\,, & t_0 < t \end{cases} \tag{1-233}$$

for the low-pass equivalent of the output. Finally, the band-pass output is obtained by using (1-222) to write

$$y_{bp}(t) = \begin{cases} [1 - \exp(-\alpha_0 t)]\cos\omega_c t & , \quad 0 \le t \le t_0 \\ [\exp(\alpha_0 t_0) - 1]\exp(-\alpha_0 t)\cos\omega_c t\,, & t_0 < t \end{cases}. \tag{1-234}$$

Figure 1-39 depicts an example plot of the response described by (1-234) when α_0 = 31.831, ω_c =

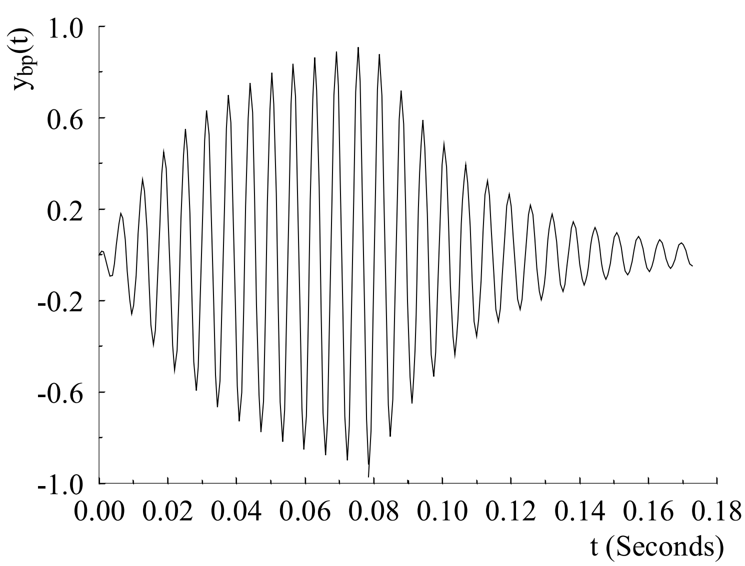

Figure 1-39: Response of LC band-pass filter to a gated sinusoid for the case α_0 = 31.831, ω_c = 1000 and t_0 = .079..

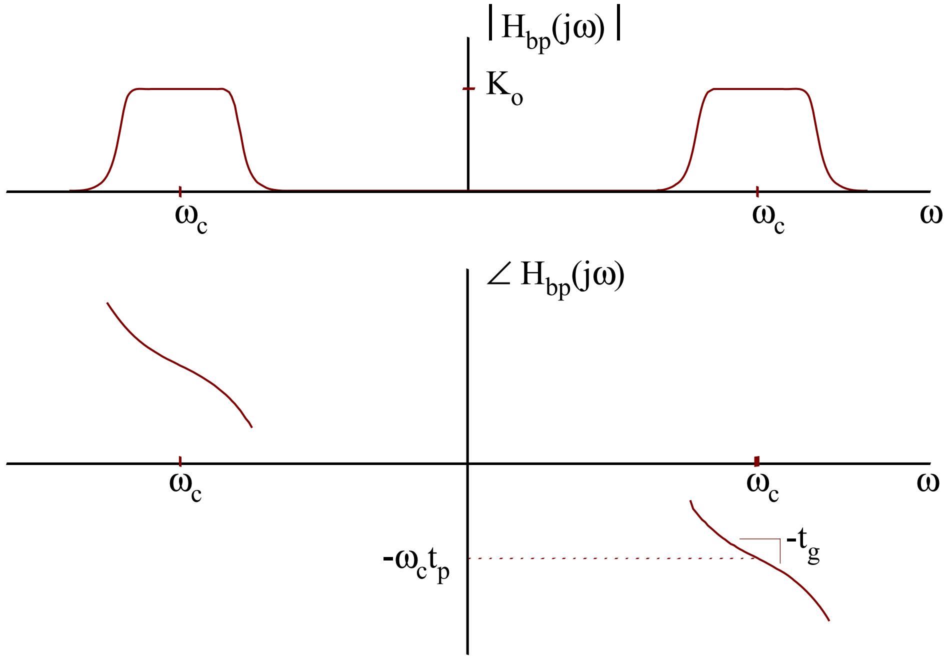

Figure 1-40: Phase delay t_p and group delay t_g of a band-pass system.

1000 and t_0 = .079.

Phase and Group Delays of a Band-Pass System

Figure 1-40 depicts the magnitude and phase response of a band-pass system with characteristics that are of interest in this section. Within the pass-band of this system, the magnitude response is almost flat and the phase response is almost linear. In addition to a bandwidth specification, times t_p and t_g can be used to characterize this system. These quantities are the subject of this section.

The quantities t_p and t_g are know as the *phase delay* and *group delay*, respectively, of the band-pass system (alternate terminology exists: Also, t_p and t_g are known as the system *carrier delay* and *envelope delay*, respectively). At center frequency ω_c, the frequency-normalized phase is $-t_p$, and $-t_g$ is the slope of the phase characteristic. In terms of the system transfer function, t_p and t_g are expressed as

$$
\begin{aligned}
t_p &\equiv -\frac{\angle H_{bp}(j\omega_c)}{\omega_c} \\
t_g &\equiv -\frac{d}{d\omega}[\angle H_{bp}(j\omega)]\Big|_{\omega=\omega_c} .
\end{aligned}
\tag{1-235}
$$

Both of these quantities have units of seconds.

A simple approximation of this band-pass system transfer function is useful in many applications. Since phase is nearly linear, it is possible to express

$$
\angle H_{bp}(j\omega) \approx -\omega_c t_p - (\omega - \omega_c) t_g \tag{1-236}
$$

for ω within the pass-band around ω_c. Likewise, since the magnitude is almost constant, the approximation

$$
\left| H_{bp}(j\omega) \right| \approx K_0 \tag{1-237}
$$

holds for ω within the pass-band. Hence, *within the pass-band* centered at ω_c, the simple approximation

$$
H_{bp}(j\omega) \approx K_0 \exp\left[-j\omega_c t_p - j(\omega - \omega_c) t_g\right] \tag{1-238}
$$

follows from (1-236) and (1-237). Finally, the low-pass equivalent of this system can be approximated as

$$
H_{lp}(j\omega) \approx 2K_0 \exp\left[-j\omega_c t_p - j\omega t_g\right] \tag{1-239}
$$

for ω *within the pass-band* of H_{lp}.

Important properties of t_p and t_g can be obtained by considering the result of applying band-pass signal

$$x_{bp}(t) = x_d(t)\cos\omega_c t \tag{1-240}$$

to the system. Assume that x_{bp} fits within the filter pass-band; that is, $X_{bp}(j\omega) \equiv \mathcal{F}[x_{bp}]$ is approximately zero outside of the nearly flat pass-band of H_{bp}. The low-pass equivalent of the filter output can be approximated (see (1-229)) as

$$\begin{aligned} Y_{lp}(j\omega) &= \frac{1}{2}H_{lp}(j\omega)X_{lp}(j\omega) \\ &\approx \frac{1}{2}\Big[2K_0\exp[-j(\omega_c t_p + \omega t_g)]X_d(j\omega)\Big], \end{aligned} \tag{1-241}$$

where $X_{lp}(j\omega) = X_d(j\omega) \equiv \mathcal{F}[x_d]$. In the time domain, the inverse of (1-241) is

$$y_{lp}(t) \approx K_0\exp(-j\omega_c t_p)\,x_d(t-t_g), \tag{1-242}$$

and the band-pass output of the filter is approximated as

$$y_{bp}(t) = \mathrm{Re}[\,y_{lp}(t)\exp(j\omega_c t)] \approx K_0\,x_d(t-t_g)\cos\omega_c[t-t_p]\,. \tag{1-243}$$

Comparison of (1-240) and (1-243) reveals why t_p and t_g are known as the system carrier delay and envelope delay, respectively.